Electronic Supplementary Information ESI

Table of contents

Diffusion NMR experiments

Diffusion NMR experiments were performed on a Bruker Avance *NEO* 600 FT NMR spectrometer, operating at a ^{1}H resonance frequency of 600.13 MHz. The instrument was equipped with a 5 mm BBO Prodigy cryoprobe with a *z*-gradient coil providing a maximum gradient strength of 6.57 G mm^{-1} at 10 A. Diffusion data were recorded using the *ledbpgp2s* pulse sequence supplied by the manufacturer. Diffusion coefficients were corrected according to the diffusion coefficient of H_2O (2.299 × 10^{-9} m^2 s^{-1} at 298 K) reported in the literature.[S1] The corresponding proportional factor $D_{H2O,lit.}/D_{H2O,est.}$ was determined on a sample of acetone-*d*6 equipped with a capillary containing H_2O. The temperature unit of the instrument was calibrated according to the instrument manufacturer's manual using the temperature dependence of the proton chemical shift difference of methanol. To obtain stable temperature conditions, the sample was held in the magnet for at least one hour prior to data collection. Proton diffusion data were collected with 32k data points and a spectral width of 7200 Hz (^{1}H) and 11.400 Hz (^{19}F), respectively. The relaxation delay was set to 10 s.

The diffusion delay time (big delta, Δ) was set to 50 or 80 ms. The gradient duration time (small delta, δ/2) was set to values between 700 and 1600 μs. The gradient strength within the diffusion experiments was increased linearly in 16 steps. The diffusion data were analysed using the *T*1/*T*2 module which is part of the Bruker *TopSpin*® software package.

The standard deviation of the experimentally determined gradient-strength dependent signal intensities from the fitted decay function was ≤ 6.2 × 10^{-3}. DOSY-Plots were generated using the Bruker *TopSpin*® software.

The hydrodynamic radii have been calculated by the Stokes-Einstein (SE) equation, (eq. 1)[S2] and the hydrodynamic volume have been calculated by equation for a spherical volume (eq. 2):

$$D = \frac{k_BT}{cf_s\pi\eta r_H} \quad r_H = \frac{k_BT}{cf_s\pi\eta D} \quad \text{(eq. 1)} \qquad V_H = \frac{4}{3}\pi r_H^3 \qquad \text{(eq. 2)}$$

D = diffusion constant

k_B = Boltzmann constant

T = temperature

η = viscosity

r_H = hydrodynamic radius

V_H = hydrodynamic volume

The *c*-factor was calculated according to Chen *et al.* (eq. 3):[S3]

$$c = \frac{6}{1+0.695(\frac{r_{solvent}}{r_{solute}})^{2.234}} \qquad \text{(eq. 3)}$$

$r_{solvent}$ = van der Waals-radius of the solvent
r_{solute} = van der Waals-radius of the solute

Van der Waals-radii of molecules have been calculated using a method reported by Abraham *et al.* (eq. 4):[S4]

$$V_{vdW}\,[\text{Å}] = \sum all\ atom\ contributions - 5.92N_b - 14.7R_A - 3.8R_{NR} \qquad \text{(eq. 4)}$$

N_b = number of bonds

R_A = number of aromatic rings

R_{NR} = number of non-aromatic rings

Table S1 Atom contributions used for van der Waals-radii calculations.[S5]

Atom	r_{vdW} [Å]	V_{vdW} [Å^3]
H	1.20	7.24
C	1.70	20.58
F	1.47	13.31
O	1.52	14.71
S	1.80	24.42
Si	2.10	38.79

Table S2 Determination of the f_s factor according to Perrin.[S6]

Prolate (cigar-shaped) molecules (applied for the reference compounds):	Oblate molecules
$$f_s = \frac{\sqrt{1-(\frac{b}{a})^2}}{(\frac{b}{a})^{\frac{2}{3}}\ln\frac{1+\sqrt{1-(\frac{b}{a})^2}}{(\frac{b}{a})}}$$	$$f_s = \frac{\sqrt{(\frac{b}{a})^2-1}}{(\frac{b}{a})^{\frac{2}{3}}\arctan\sqrt{(\frac{b}{a})^2-1}}$$
a: long diameter b: short diameter	a: long diameter b: short diameter

Table S3 Viscosity data of acetonitrile.[S7]

Temperature [K]	Viscosity [Pa s]
233	0.000831
243	0.000705
253	0.000592
263	0.000512
273	0.000461
283	0.000423
293	0.000389
303	0.000356
313	0.000323
323	0.000293

Samples for DOSY NMR experiments were freshly prepared by dissolving 12–15 mg of **3** in acetonitrile-d3 and then adding a corresponding portion of the guest. The exact stoichiometric ratio host:guest was determined by integrating the host and guest signals in an ^{1}H NMR spectrum prior to the measurement.

The overall error in the calculated diffusion coefficients can be estimated to be ≤ ±5%. Deviations from the SE law are expected for small molecules with radii in the range of that of the solvent exhibiting non-spherical molecular structures. Although methods have been reported to describe the hydrodynamic behaviour of such compounds by using a factor c adapted to the size and a factor fs depending on the form of the solute, it is difficult to determine the correct factors in this case, since the proportions of the individual species in equilibrium are unknown, especially for open chain and cyclic forms, for which completely different shapes can be expected. Accordingly, we calculated hydrodynamic radii according to the SE law and interpreted the data by comparison with those of suitable reference compounds. The use of reference compounds of very similar shape, treated in exactly the same way as the analyte, lead to a minimum of possible introduced errors in the factor c. Although according to eq. 2, the error in V_H increases with respect to r_H, we used V_H to determine the level of aggregation,

which facilitates the comparison with reference compounds and it allows the approximation of V_H for the proposed adducts simply by adding the corresponding volumes of the components.

Experimental diffusion NMR data

Table S4 Corrected diffusion coefficients (D_{corr}), hydrodynamic radii (r_H) and hydrodynamic volumes (V_H) derived from DOSY NMR experiments for PLA **5**, triazine, TrisPhos and the corresponding adducts **5·triazine** and **5·TrisPhos**.

Compound	D_{corr} [10^{-10} m^2 s^{-1}] host/guest	r_H (SE) [Å] host/guest	r_H (cf) [Å] host/guest	V_H (SE) [Å^3] host/guest	V_H (cf) [Å^3] host/guest
5	6.17/–	6.14/–	6.74/–	967/–	1284/–
triazine	18.65/–	2.03/–	3.20/–	35/–	138/–
TrisPhos	9.14/–	4.14/–	4.95/–	298/–	508/–
5·triazine	5.54/7.16	6.83/5.29	7.47/5.78	1335/620	1743/809
5·TrisPhos	5.25/5.37	7.22/7.04	7.77/7.59	1574/1463	1967/1829

Table S5 Corrected diffusion coefficients (D_{corr}), hydrodynamic radii (r_H) and hydrodynamic volumes (V_H) derived from DOSY NMR experiments for the free PLA and the adduct **3·[3pPhpy]** (1/6.90). The data is determined *via* ^{1}H DOSY NMR.

Compound molar ratio (host/guest)	D_{corr} [10^{-10} m^2 s^{-1}]	r_H (SE) [Å]	V_H [Å^3] (SE)
3 (1/0)	8.74	6.31	1053
3·[3pPhpy] (1/6.90)	7.49	7.43	1720

Table S6 Corrected diffusion coefficients (D_{corr}), hydrodynamic radii (r_H) and hydrodynamic volumes (V_H) derived from DOSY NMR experiments for the adduct of **3** with 3,3'-bipyridine at different guest concentrations.

Molar ratio (host/guest)	D_{corr} [10^{-10} m^2 s^{-1}] host/guest/triflate	r_H (SE) [Å] host/guest/triflate	V_H [Å^3] (SE) host/guest/triflate
1/0.13	8.42	6.55/4.75/5.58	1176/448/726
1/0.31	8.10	6.81/5.96/5.37	1323/885/647
1/0.53	7.93	6.95/6.39/5.13	1408/1092/565
1/1.30	6.54	8.43/7.52/4.51	2512/1778/383
1/1.99	6.68	8.26/6.58/4.03	2356/1192/274
1/2.13	6.31	8.74/6.69/4.07	2797/1254/282
1/2.35	6.66	8.28/6.12/3.90	2376/960/248
1/3.16	6.73	8.20/5.07/3.77	2309/546/224
1/6.69	6.73	8.20/3.66/3.88	2307/206/244

DOSY Plots
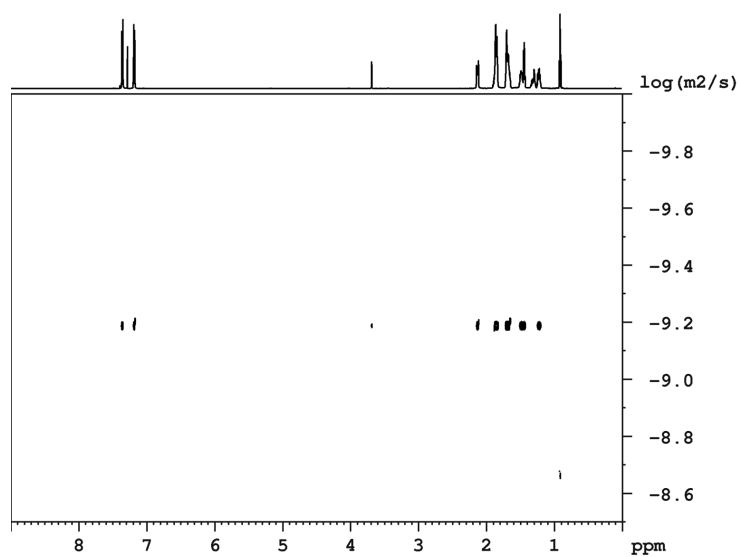
Figure S1 DOSY plot of **5** in CDCl$_3$ at 293 K.
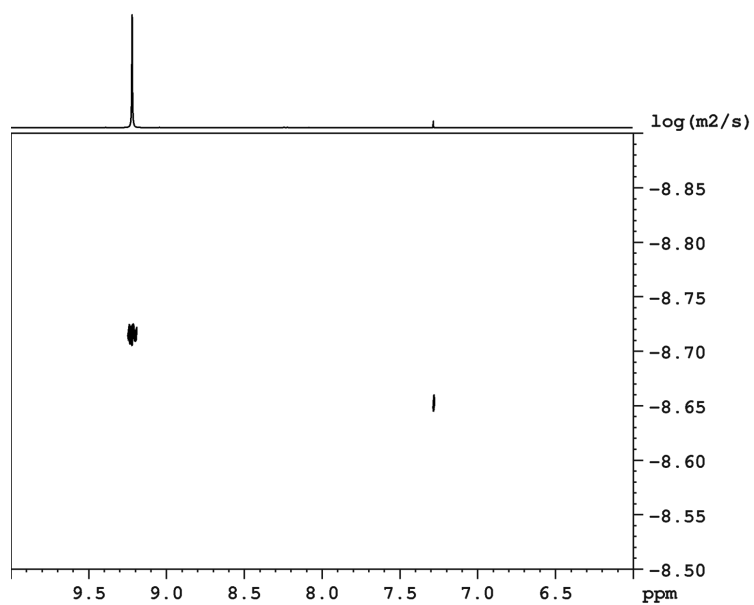
Figure S2 DOSY plot of triazine in CDCl$_3$ at 293 K.
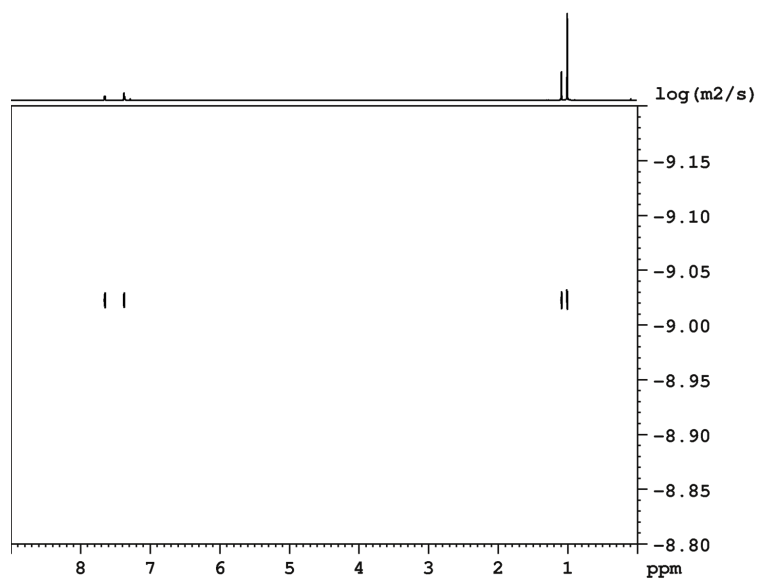
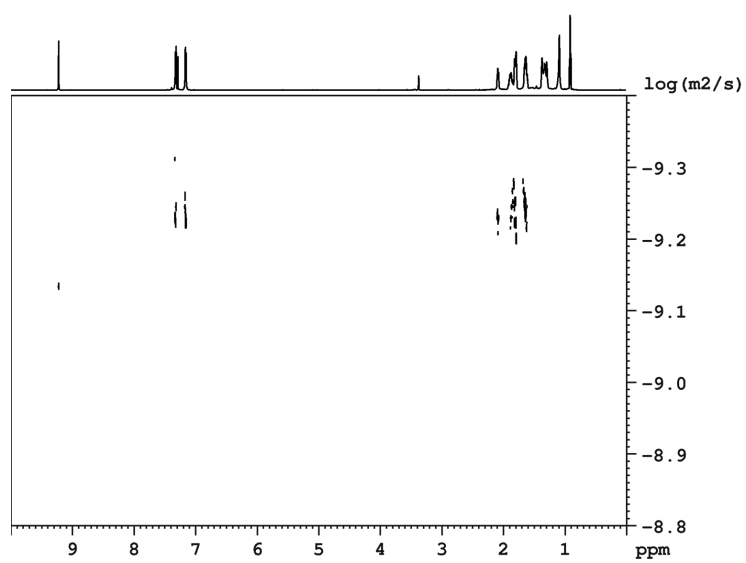**Figure S3** DOSY plot of TrisPhos in CDCl₃ at 293 K.

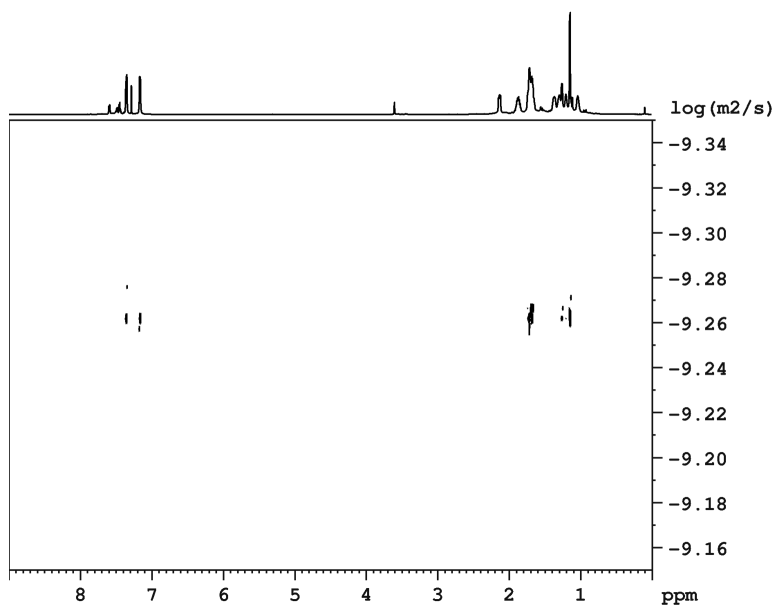**Figure S4** DOSY plot of **5**·triazine in CDCl₃ at 293 K.

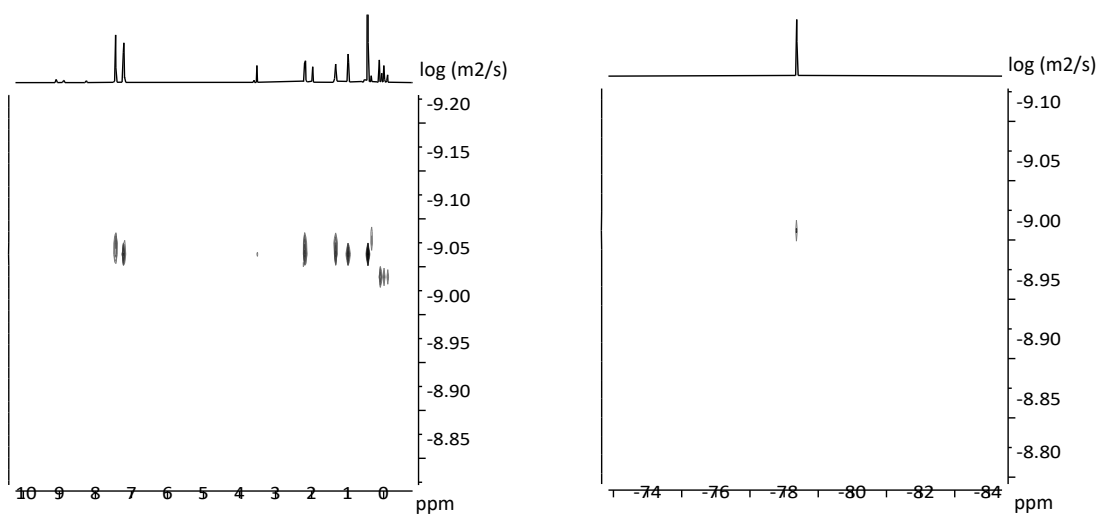**Figure S5** DOSY plot of **5**·TrisPhos in CDCl₃ at 293 K.

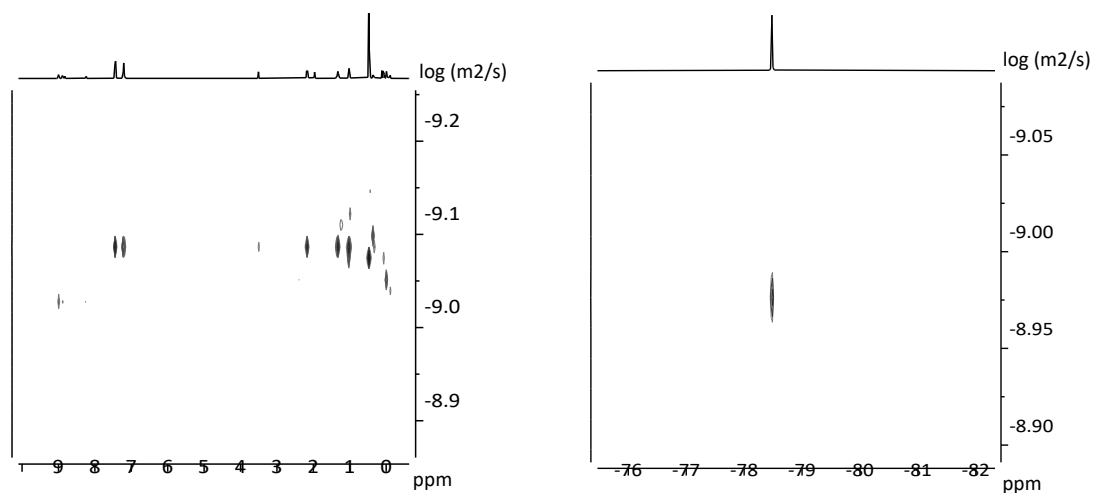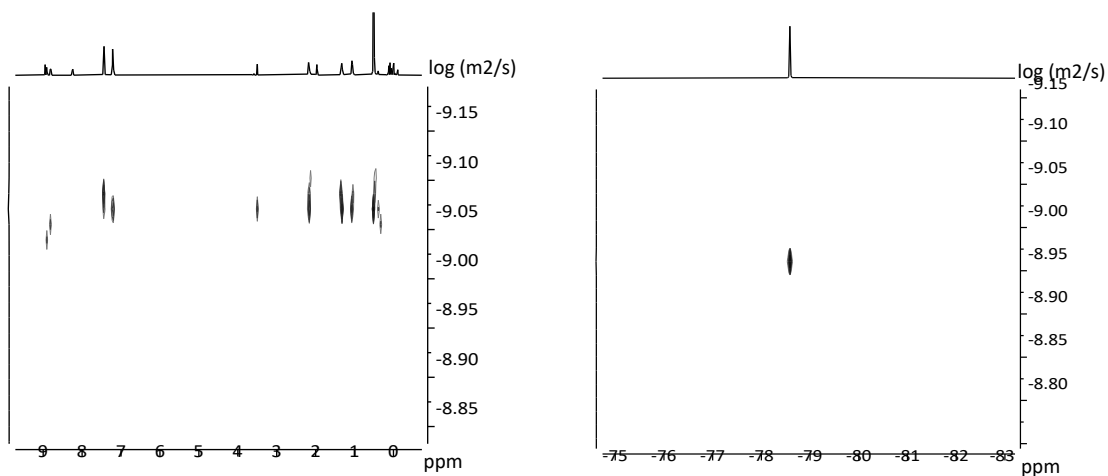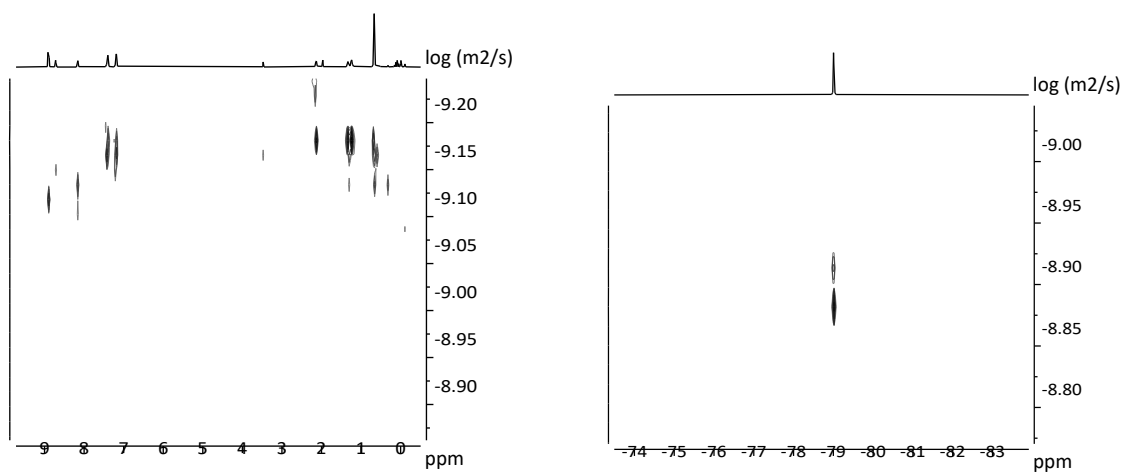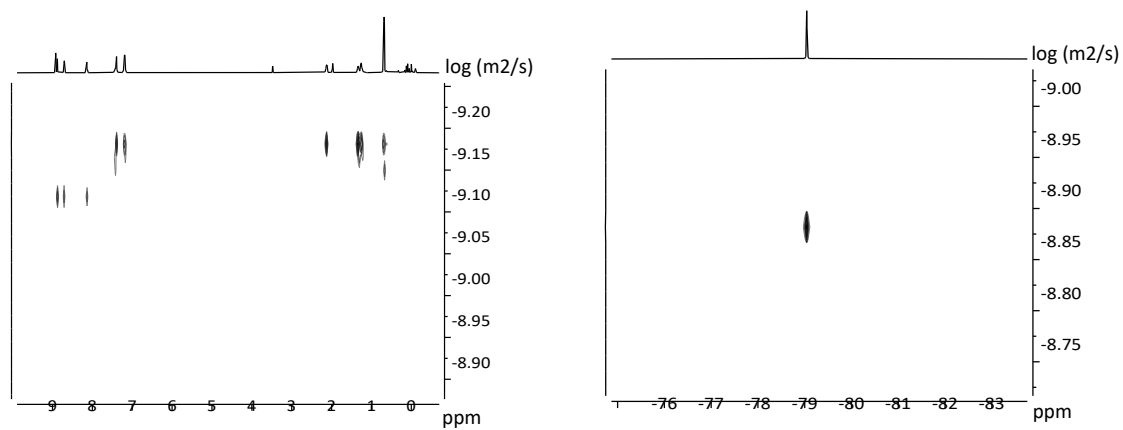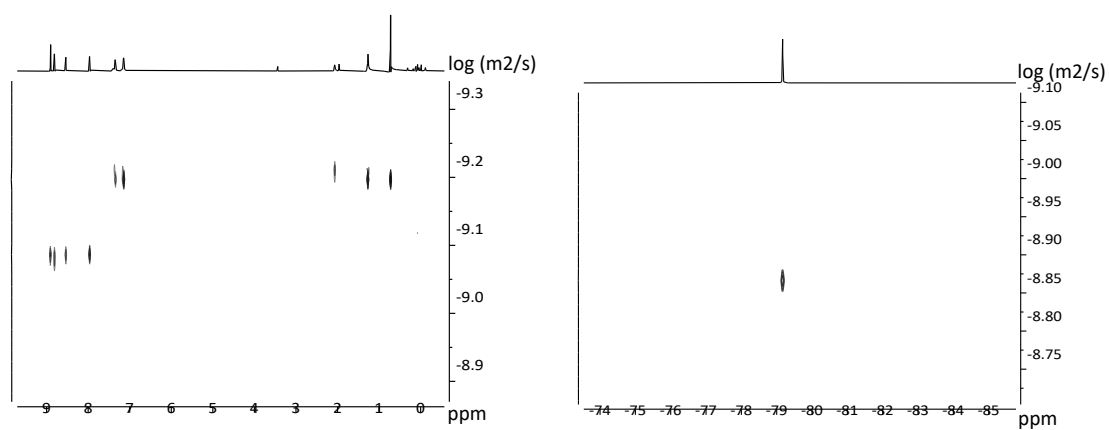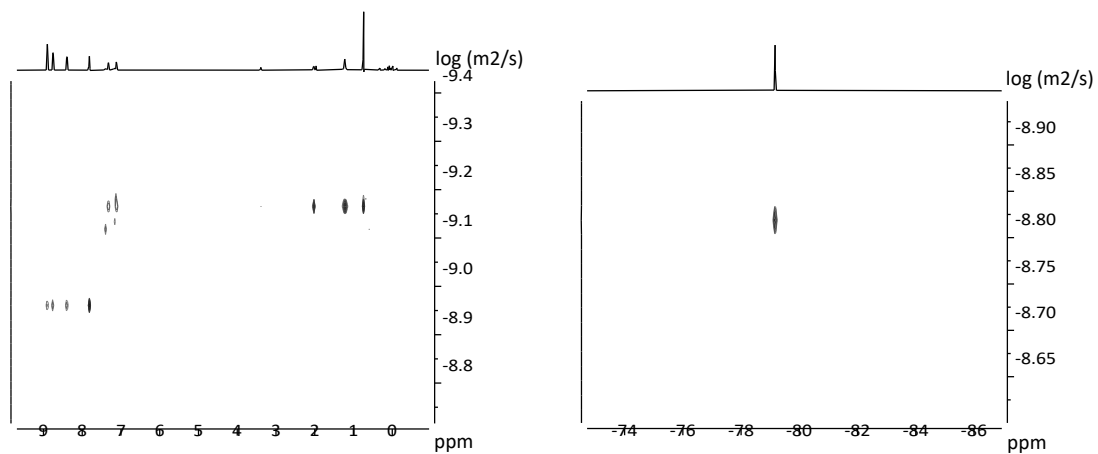**Figure S6** ¹H and ¹⁹F DOSY plots of **3** and 0.13 eq. 3,3'-bipyridine in CD₃CN at 293 K.

Figure S7 ^{1}H and ^{19}F DOSY plots of **3** and 0.31 eq. 3,3'-Bipyridine in CD$_3$CN at 293 K.

Figure S8 ^{1}H and ^{19}F DOSY plots of **3** and 0.53 eq. 3,3'-bipyridine in CD$_3$CN at 293 K.

Figure S9 ^{1}H and ^{19}F DOSY plots of **3** and 1.3 eq. 3,3'-bipyridine in CD$_3$CN at 293 K.

8

Figure S10 ^{1}H and ^{19}F DOSY plots of **3** and 1.99 eq. 3,3'-bipyridine in CD$_3$CN at 293 K.

Figure S11 ^{1}H and ^{19}F DOSY plots of **3** and 2.13 eq. 3,3'-bipyridine in CD$_3$CN at 293 K.
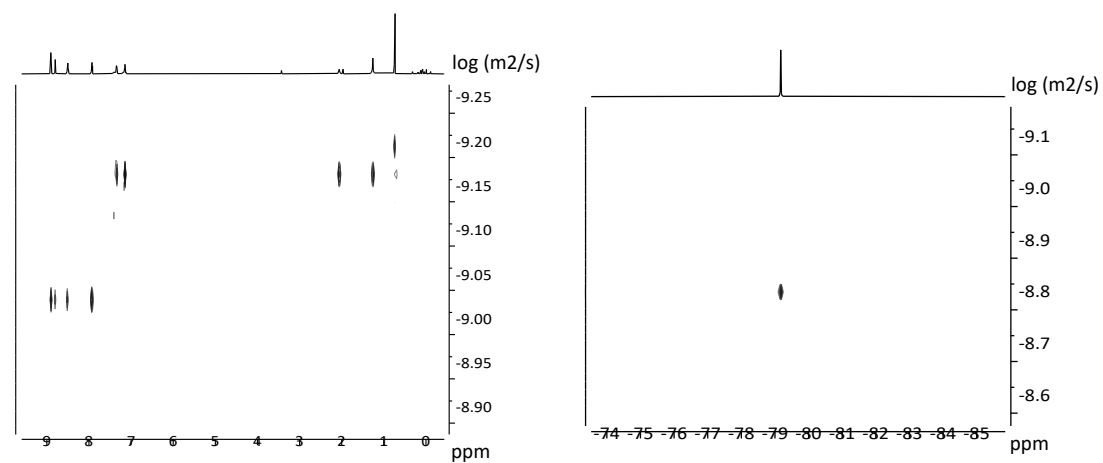
Figure S12 ^{1}H and ^{19}F DOSY plots of **3** and 2.35 eq. 3,3'-bipyridine in CD$_3$CN at 293 K.

Figure S13 ^{1}H and ^{19}F DOSY plots of **3** and 3.16 eq. 3,3'-bipyridine in CD$_3$CN at 293 K.
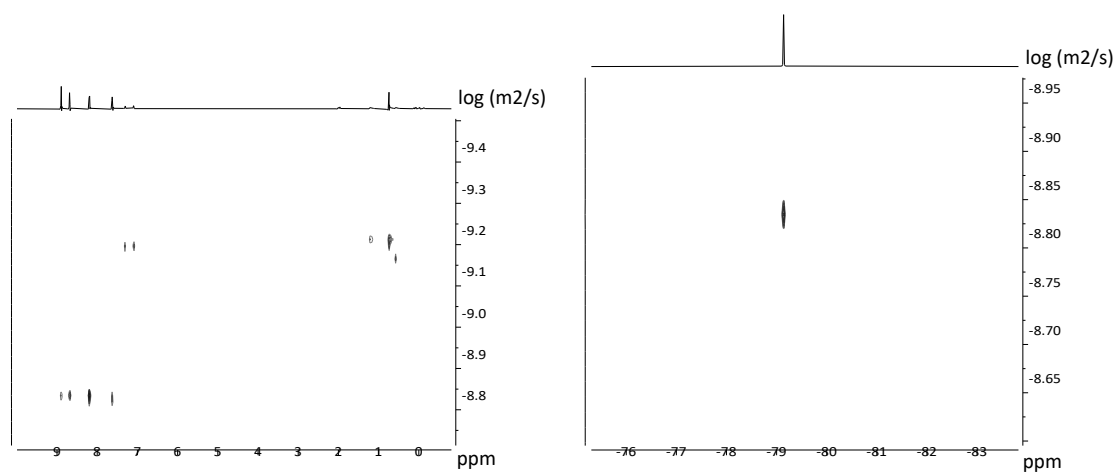
Figure S14 ^{1}H and ^{19}F DOSY plots of **3** and 6.69 eq. 3,3'-bipyridine in CD$_3$CN at 293 K.

NMR spectroscopic data
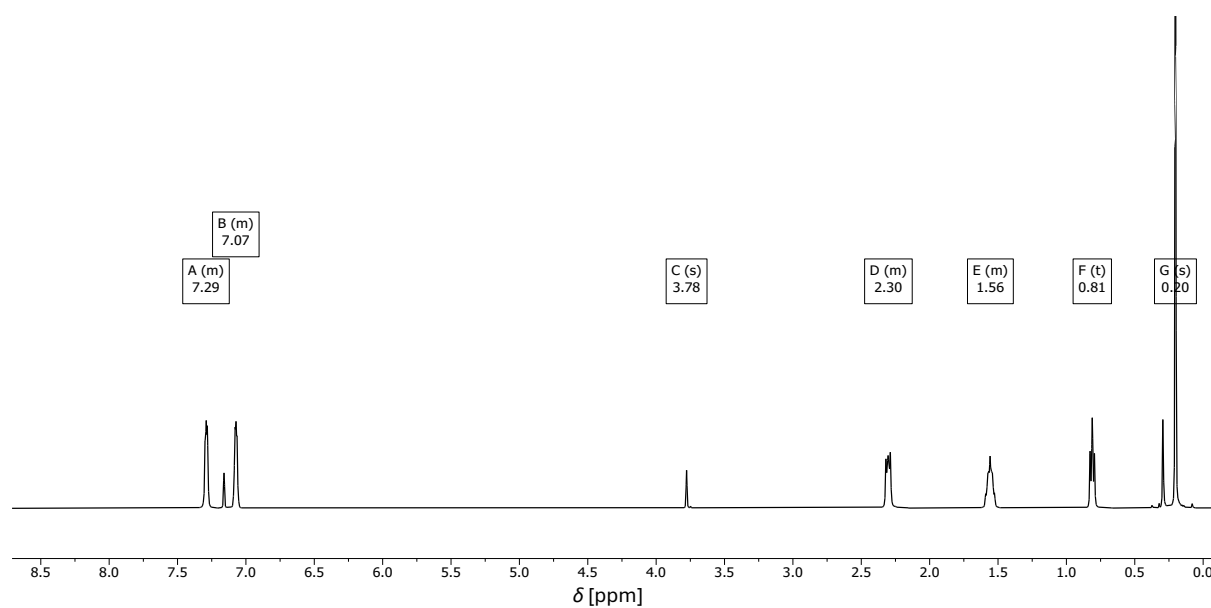
Figure S15 ^{1}H NMR spectrum of a solution of 4b,8b,12b-tris(3-(chloro(dimethyl)silyl)propyl)tribenzotriquinacene **2** in C$_6$D$_6$ (500 MHz, 298 K).
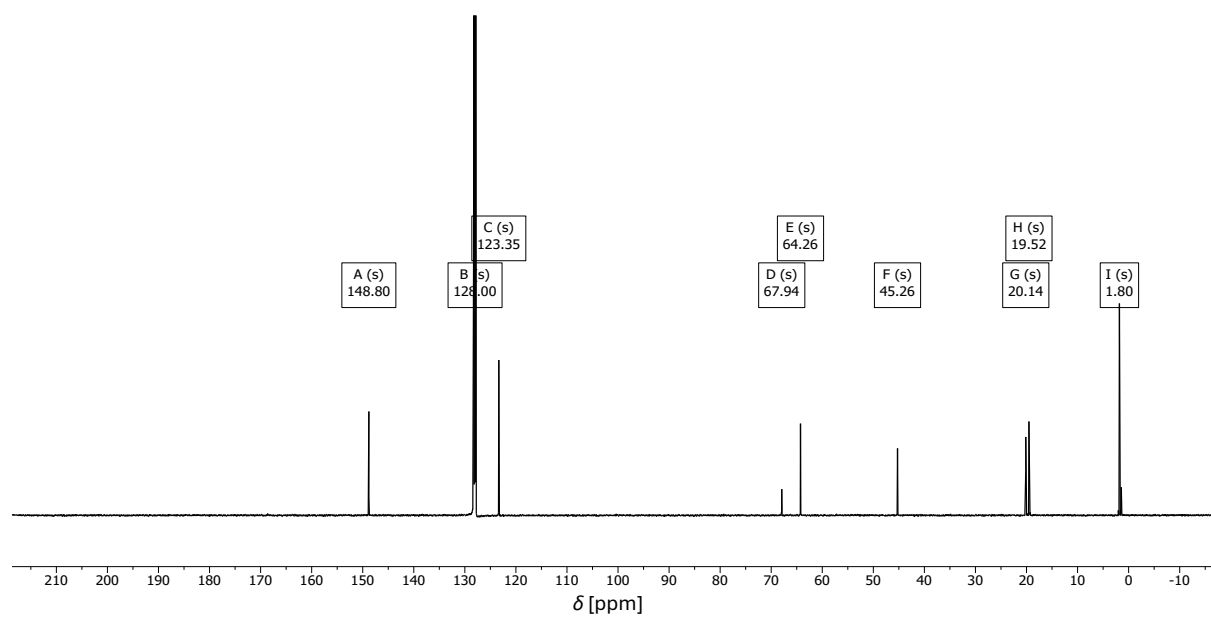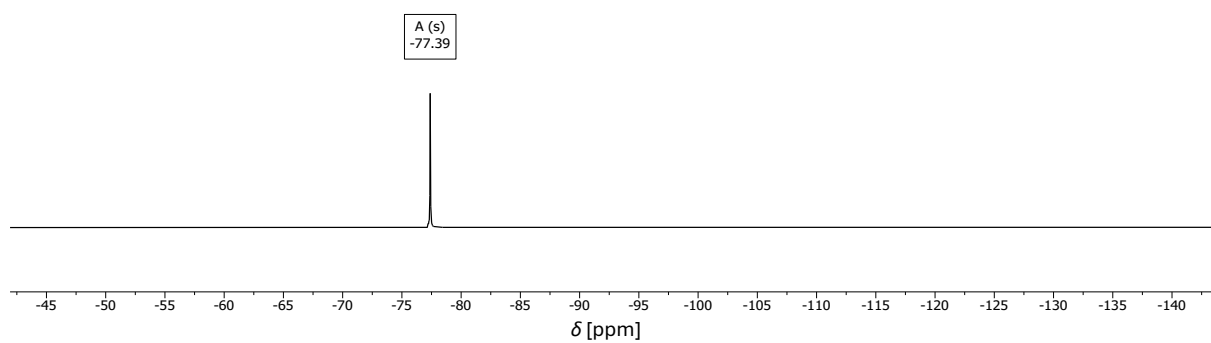

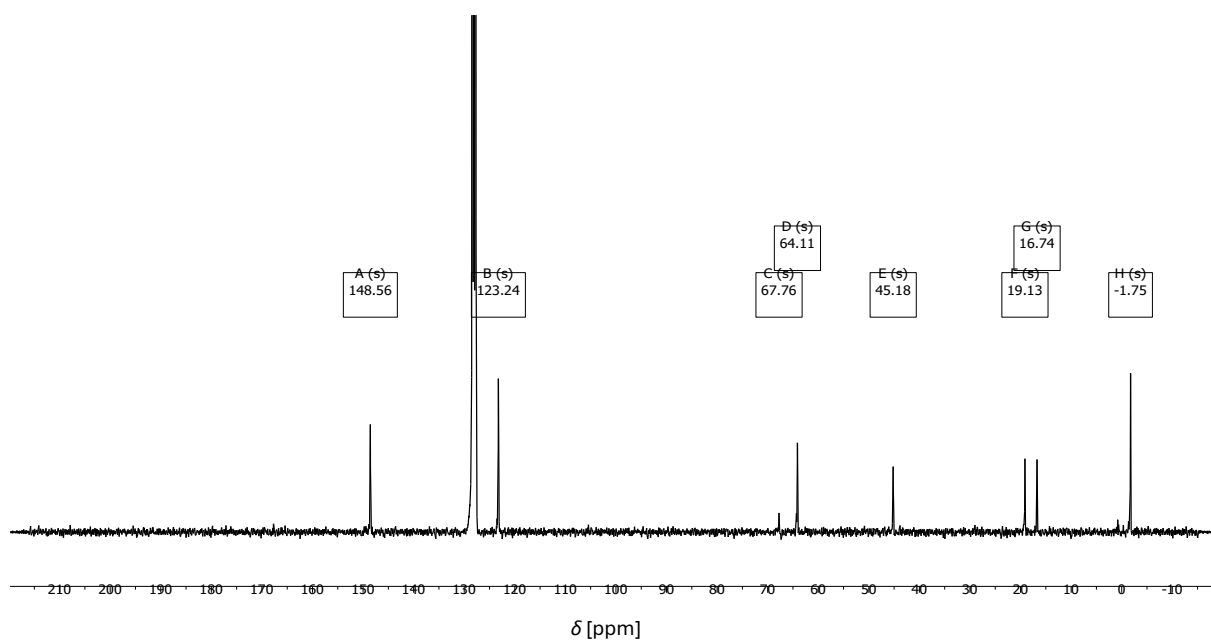**Figure S16** ^{13}C{^{1}H} NMR spectrum of a solution of 4b,8b,12b-tris(3-(chloro(dimethyl)silyl)propyl)tribenzotriquinacene **2** in C$_6$D$_6$ (126 MHz, 298 K).
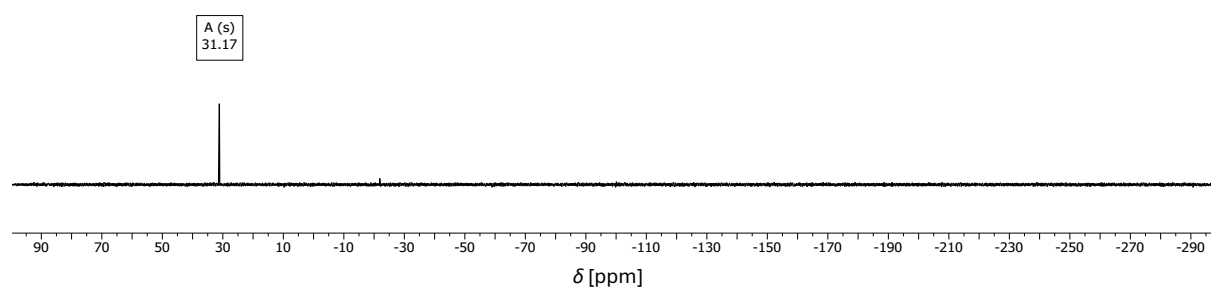
Figure S17 ^{29}Si{^{1}H} NMR spectrum of a solution of 4b,8b,12b-tris(3-(chloro(dimethyl)silyl)propyl)tribenzotriquinacene **2** in C$_6$D$_6$ (99 MHz, 298 K).
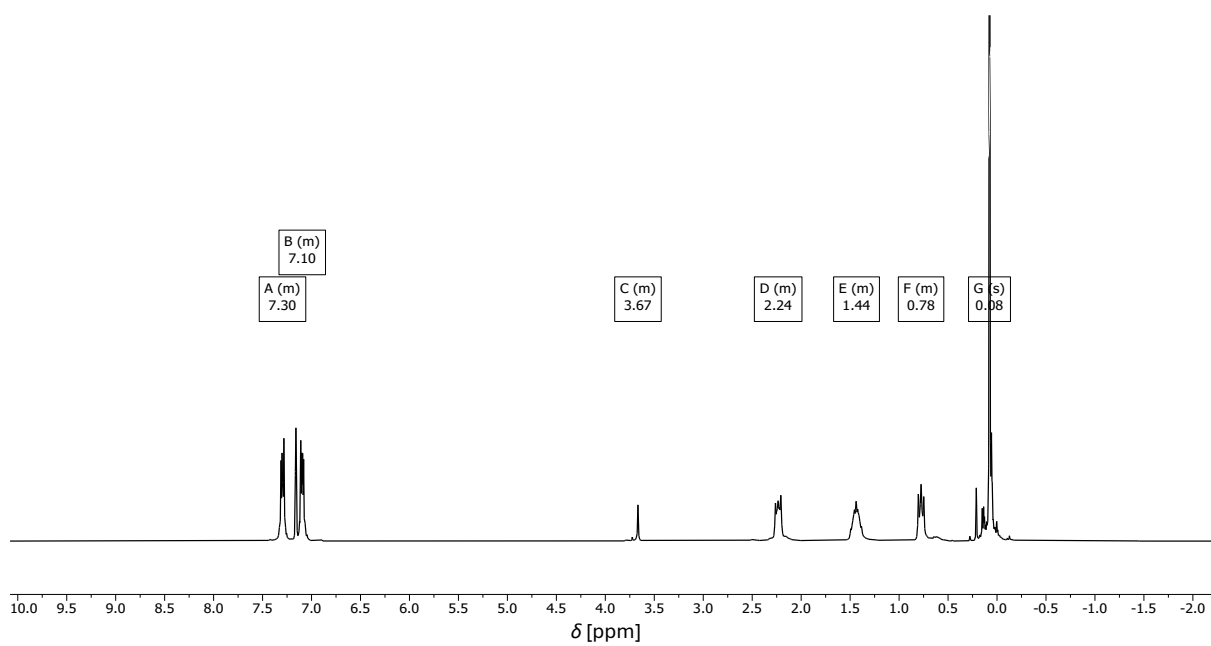
Figure S18 ¹H NMR spectrum of a solution of 4b,8b,12b-tris(3-(trifluoromethylsulfonyl(dimethyl)silyl)propyl)tribenzotriquinacene **3** in C₆D₆ (500 MHz, 298 K).

Figure S19 ¹⁹F NMR spectrum of a solution of 4b,8b,12b-tris(3-(trifluoromethylsulfonyl(dimethyl)silyl)propyl)tribenzotriquinacene **3** in C₆D₆ (282 MHz, 298 K).
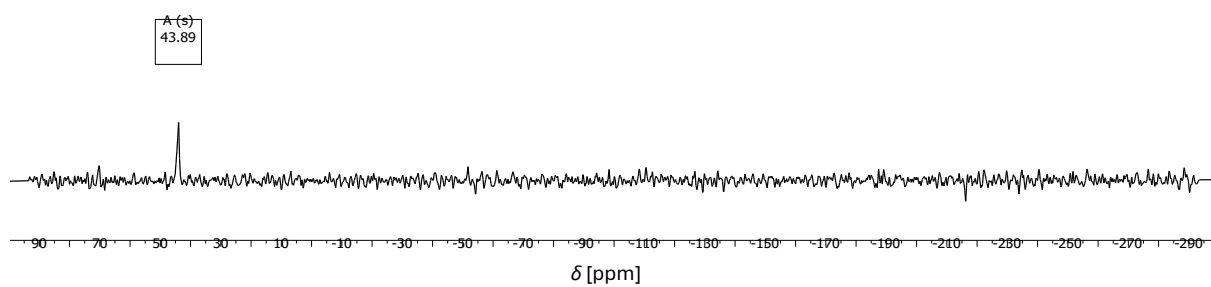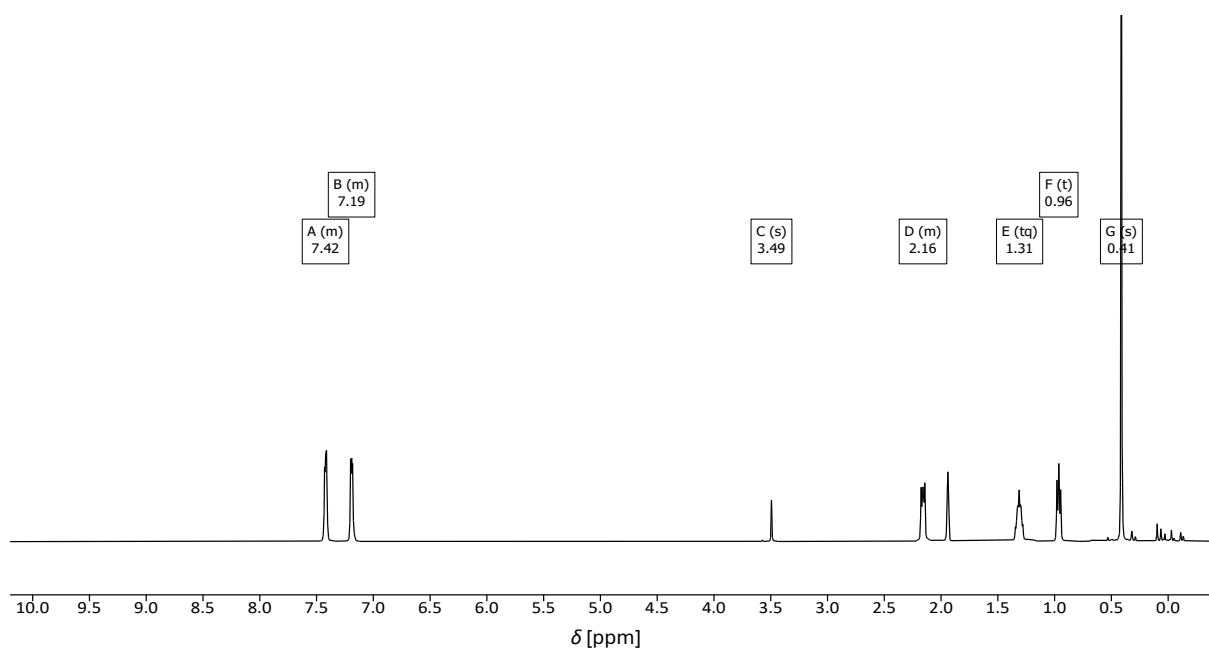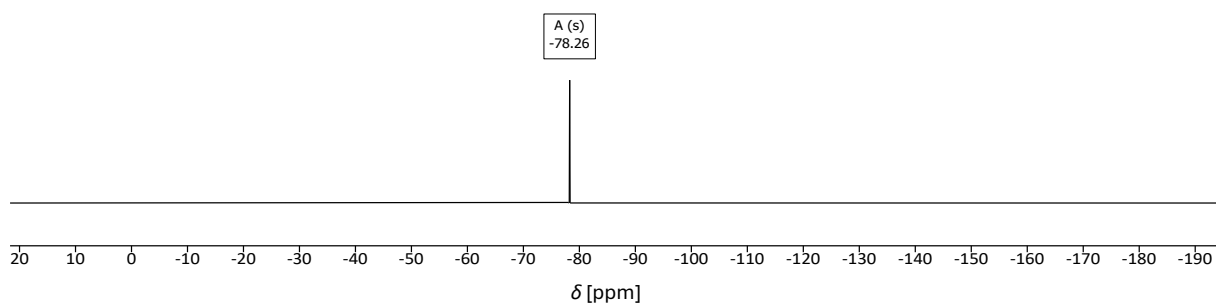
Figure S20 $^{13}C\{^1H\}$ NMR spectrum of a solution of 4b,8b,12b-tris(3-(trifluoromethylsulfonyl(dimethyl)silyl)propyl)tribenzotriquinacene **3** in C_6D_6 (75 MHz, 298 K).
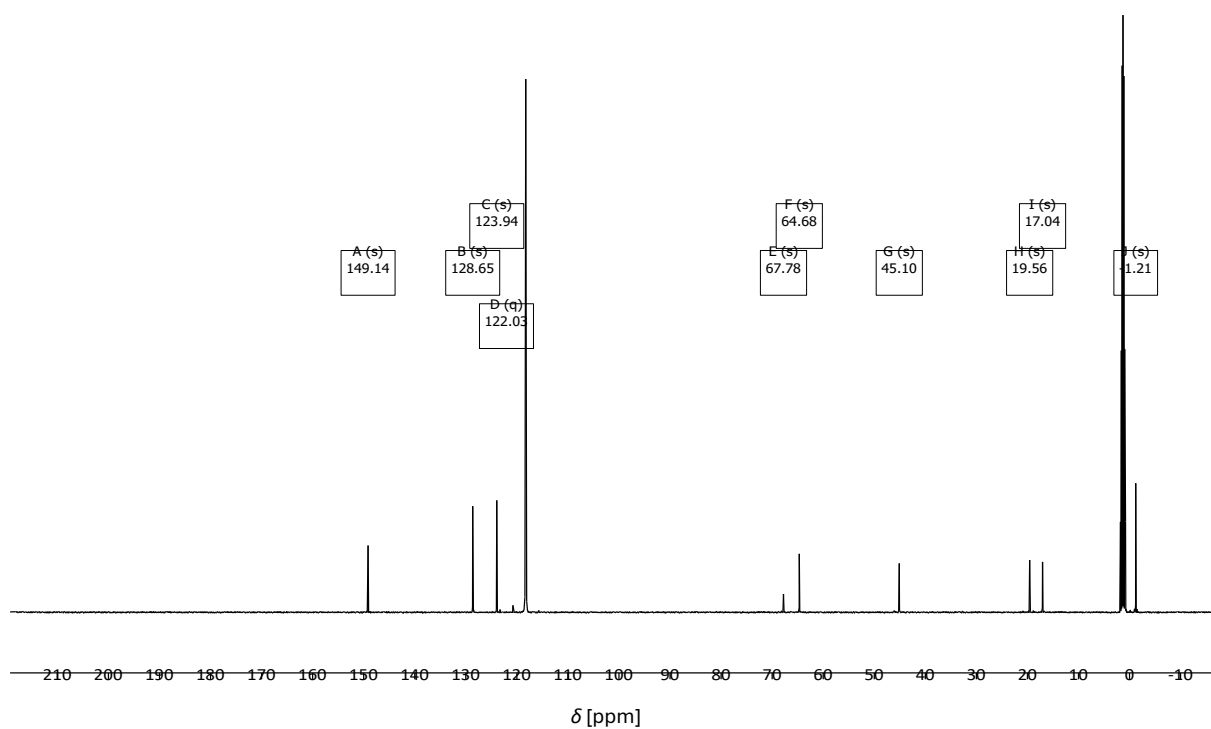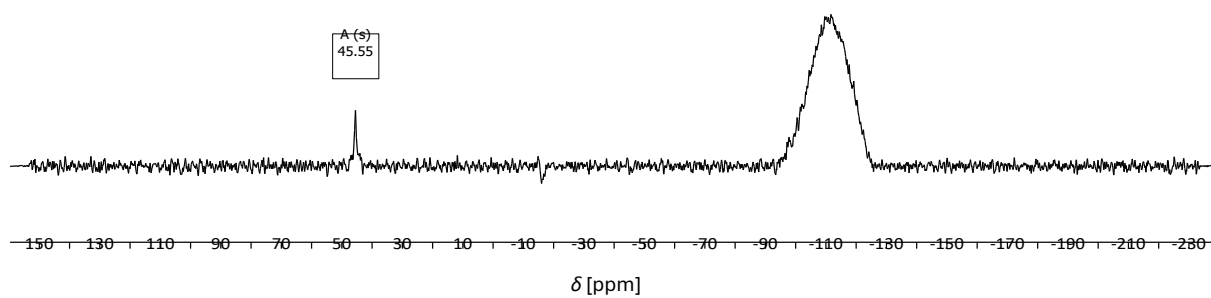

Figure S21 ^{19}F NMR spectrum of a solution of 4b,8b,12b-tris(3-(trifluoromethylsulfonyl(dimethyl)silyl)propyl)tribenzotriquinacene **3** in C_6D_6 (99 MHz, 298 K).
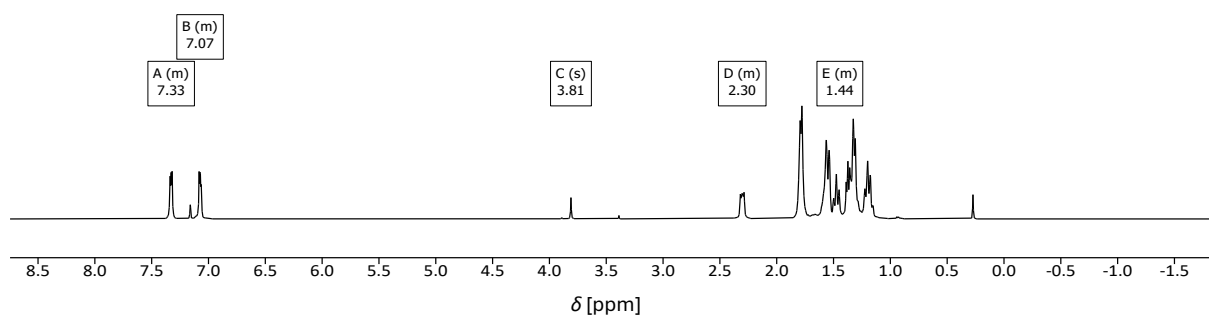
Figure S22 ¹H NMR spectrum of a solution of 4b,8b,12b-tris(3-(trifluoromethylsulfonyl(dimethyl)silyl)propyl)tribenzotriquinacene **3** in CD₃CN (500 MHz, 298 K).

Figure S23 ¹⁹F NMR spectrum of a solution of 4b,8b,12b-tris(3-(trifluoromethylsulfonyl(dimethyl)silyl)propyl)tribenzotriquinacene **3** in CD₃CN (471 MHz, 298 K).

Figure S24 $^{13}C\{^1H\}$ NMR spectrum of a solution of 4b,8b,12b-tris(3-(trifluoromethylsulfonyl(dimethyl)silyl)propyl)tribenzotriquinacene **3** in CD$_3$CN (126 MHz, 298 K).

Figure S25 $^{29}Si\{^1H\}$ NMR spectrum of a solution of 4b,8b,12b-tris(3-(trifluoromethylsulfonyl(dimethyl)silyl)propyl)tribenzotriquinacene **3** in CD$_3$CN (99 MHz, 298 K).

15

Figure S26 ^{1}H NMR spectrum of a solution of 4b,8b,12b-tris(3-(dicyclohexylboryl)propyl)tribenzotriquinacene **4** in C_6D_6 (500 MHz, 298 K).
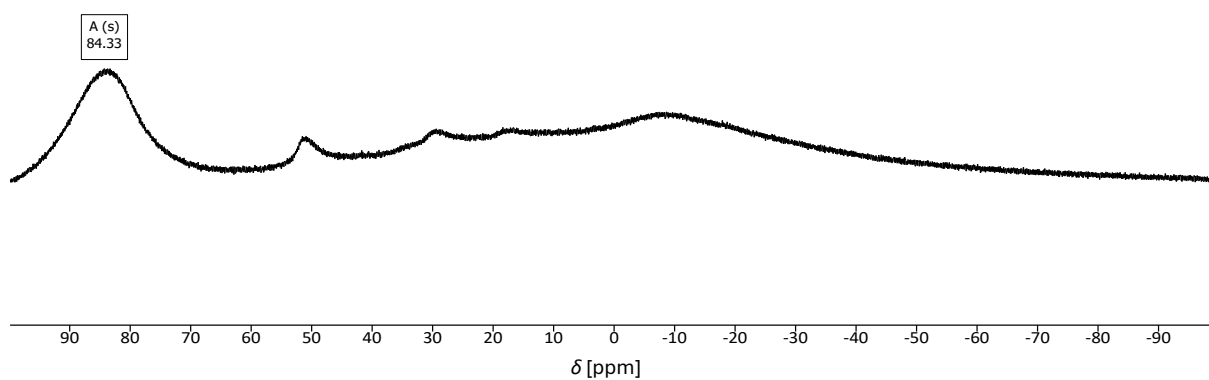
Figure S27 ^{11}B NMR spectrum of a solution of 4b,8b,12b-tris(3-(dicyclohexylboryl)propyl)tribenzotriquinacene **4** in C_6D_6 (160 MHz, 298 K).
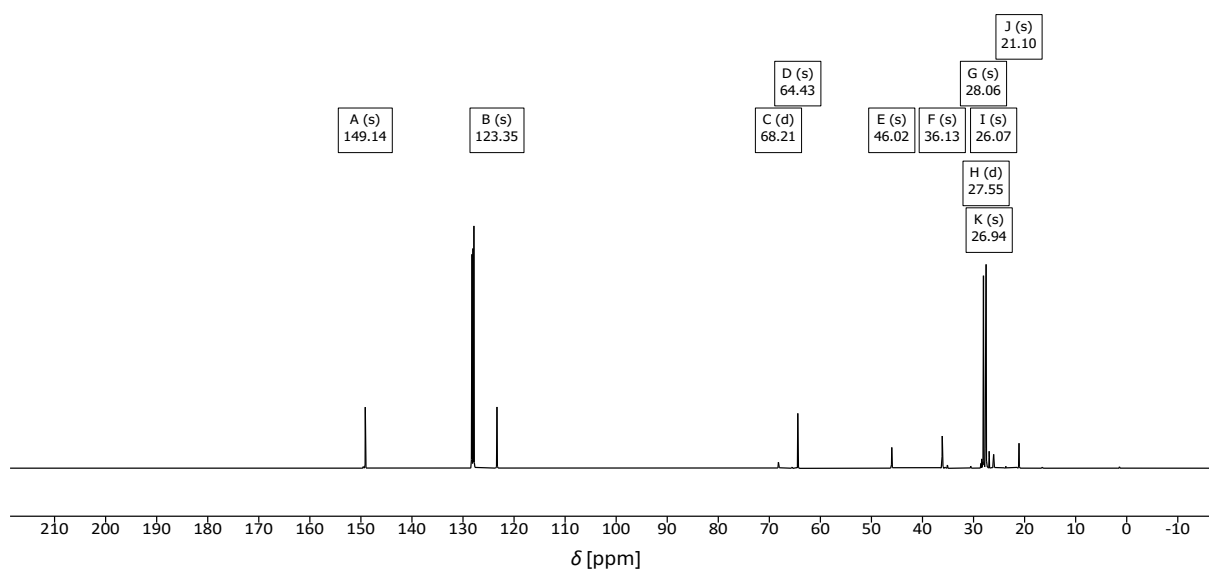

Figure S28 ^{13}C{^{1}H} NMR spectrum of a solution of 4b,8b,12b-tris(3-(dicyclohexylboryl)propyl)tribenzotriquinacene **4** in C_6D_6 (126 MHz, 298 K).
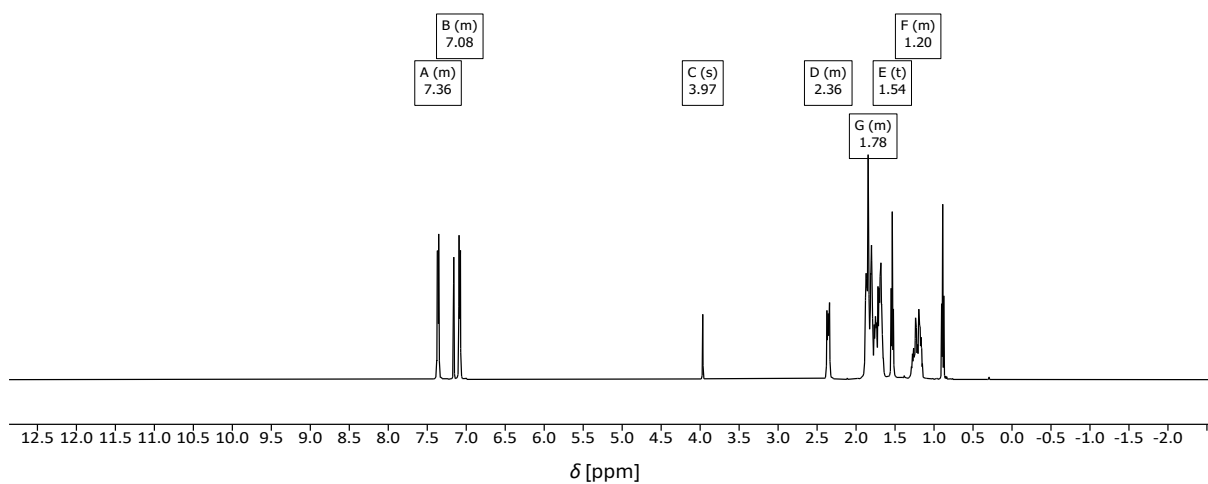
Figure S29 ^{1}H NMR spectrum of a solution of 4b,8b,12b-tris(3-(9-borabicyclo[3.3.1]nonanyl)propyl)tribenzotriquinacene **5** in C$_6$D$_6$ (500 MHz, 298 K).
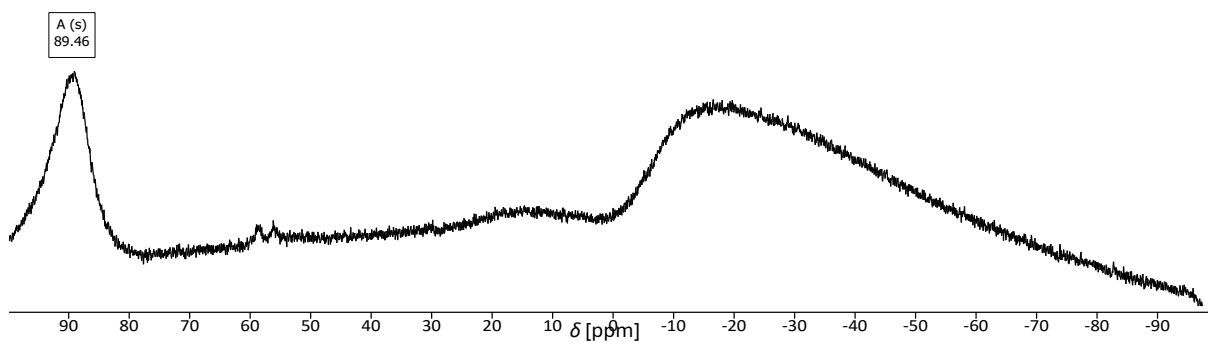

Figure S30 ^{11}B NMR spectrum of a solution of 4b,8b,12b-tris(3-(9-borabicyclo[3.3.1]nonanyl)propyl)tribenzotriquinacene **5** in C$_6$D$_6$ (160 MHz, 298 K).
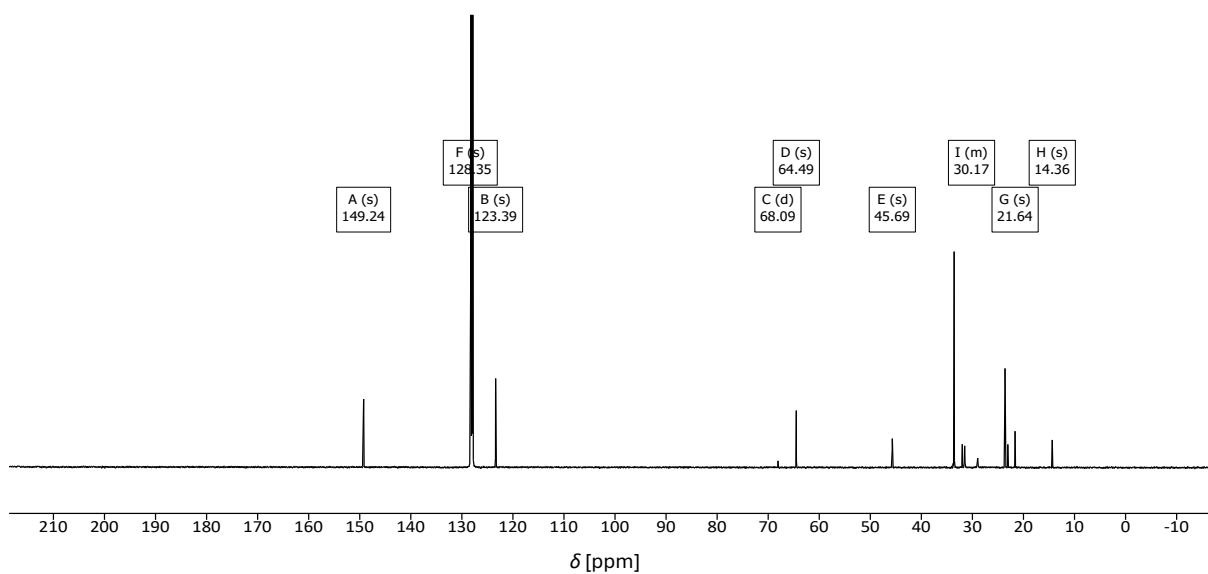

Figure S31 ^{13}C{^{1}H} NMR spectrum of a solution of 4b,8b,12b-tris(3-(9-borabicyclo[3.3.1]nonanyl)propyl)tribenzotriquinacene **5** in C$_6$D$_6$ (126 MHz, 298 K).
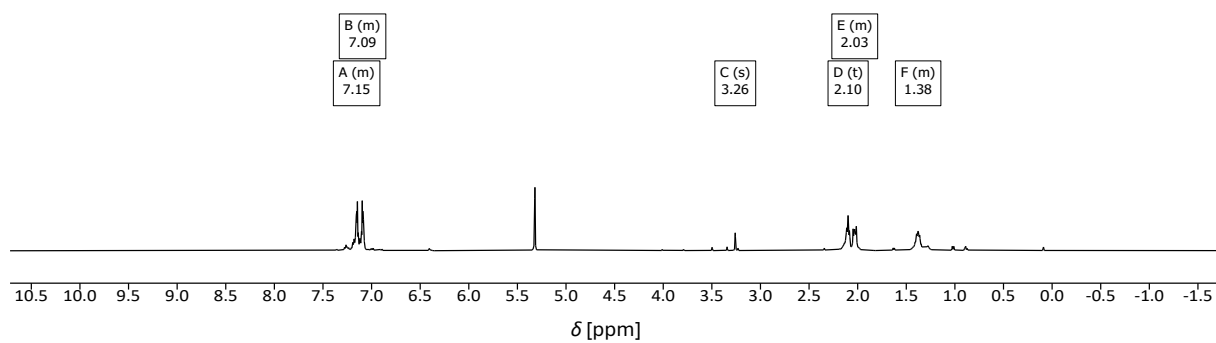
Figure S32 ¹H NMR spectrum of a solution of 4b,8b,12b-tris(3-(bis(pentafluorophenyl)boryl)propyl)tribenzotriquinacene **6** in CD₂Cl₂ (500 MHz, 298 K).
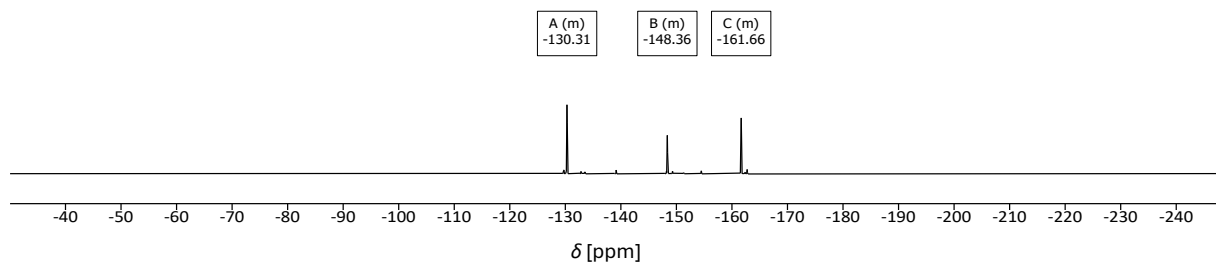

Figure S33 ¹⁹F NMR spectrum of a solution of 4b,8b,12b-tris(3-(bis(pentafluorophenyl)boryl)propyl)tribenzotriquinacene **6** in CD₂Cl₂ (471 MHz, 298 K).
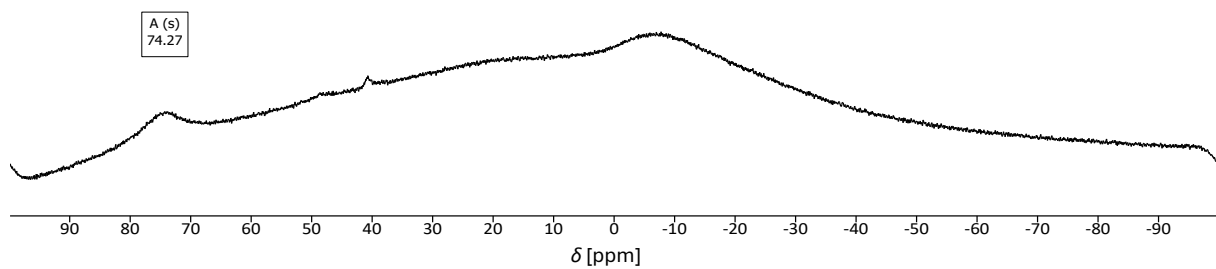

Figure S34 ¹¹B NMR spectrum of a solution of 4b,8b,12b-tris(3-(bis(pentafluorophenyl)boryl)propyl)tribenzotriquinacene **6** in CD₂Cl₂ (160 MHz, 298 K).

Figure S35 ^{13}C{^{1}H} NMR spectrum of a solution of 4b,8b,12b-tris(3-(bis(pentafluorophenyl)boryl)propyl)tribenzotriquinacene **6** in CD$_2$Cl$_2$ (126 MHz, 298 K).
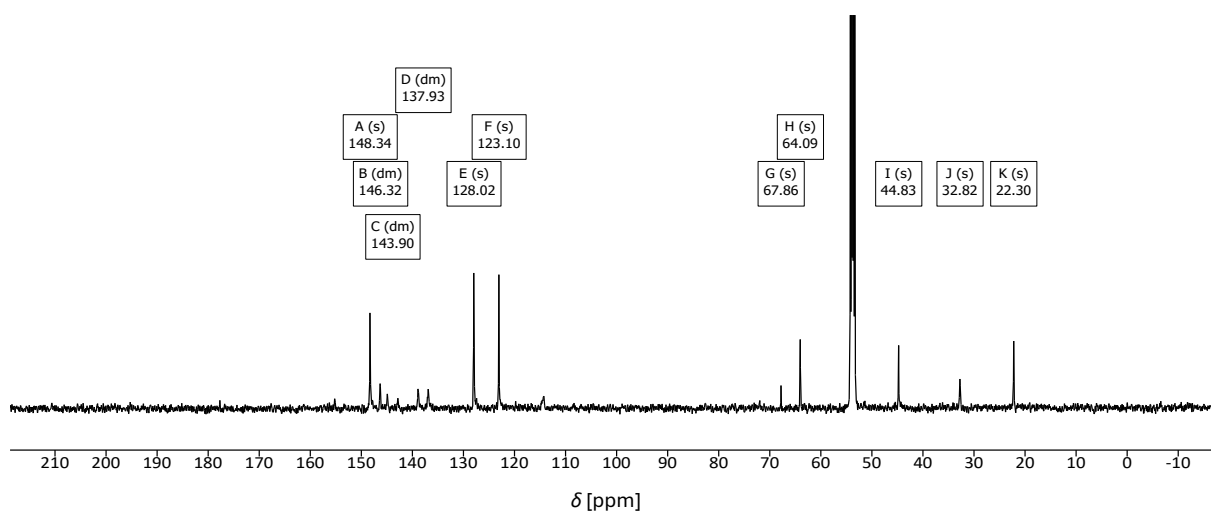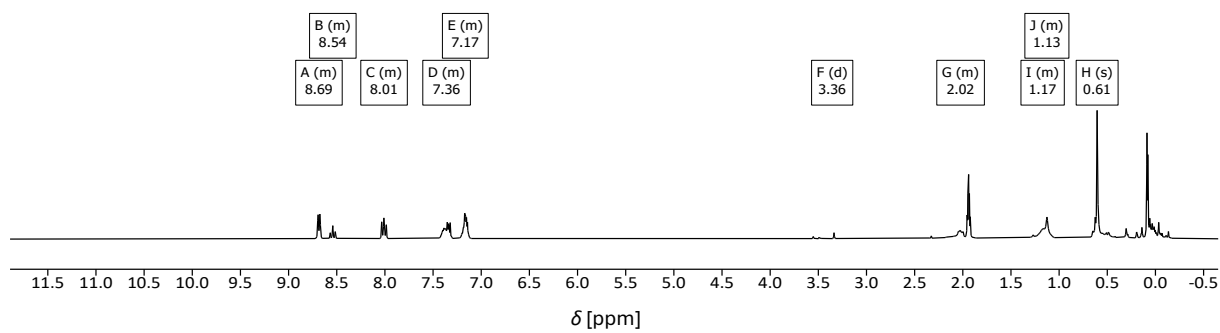

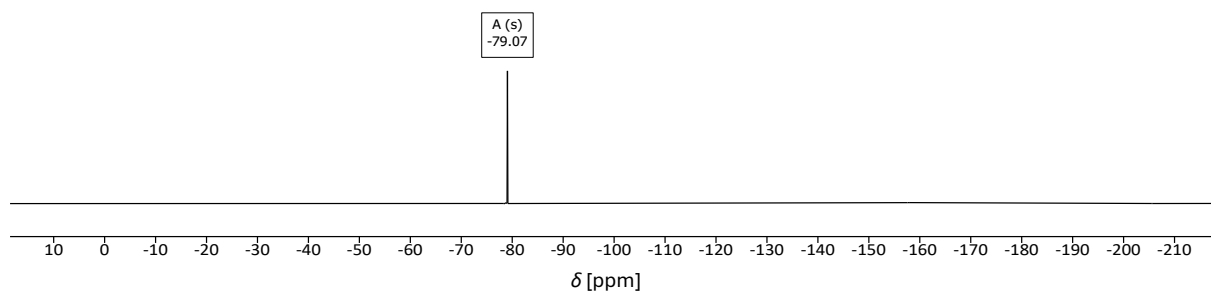**Figure S36** ^{1}H NMR of a solution of **3**·3Py in CD$_3$CN (300 MHz, 298 K).

Figure S37 ^{19}F NMR of a solution of **3**·3Py in CD$_3$CN (282 MHz, 298 K).
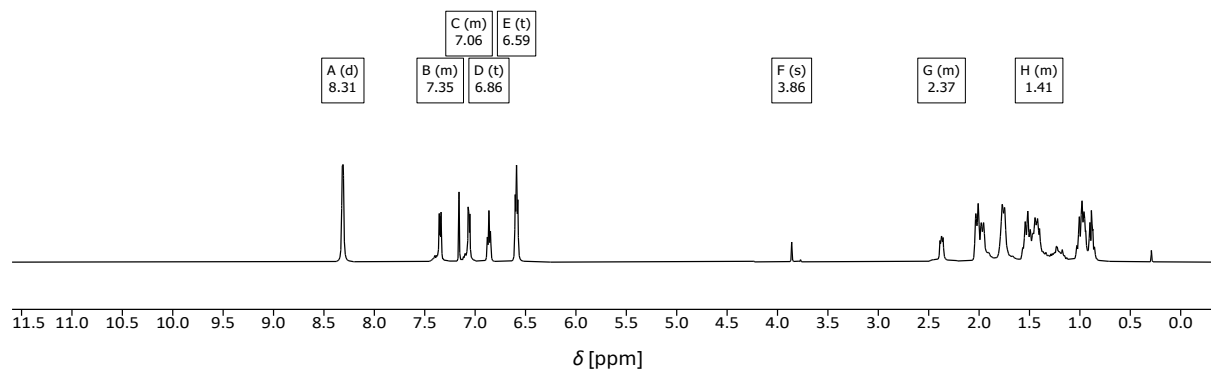
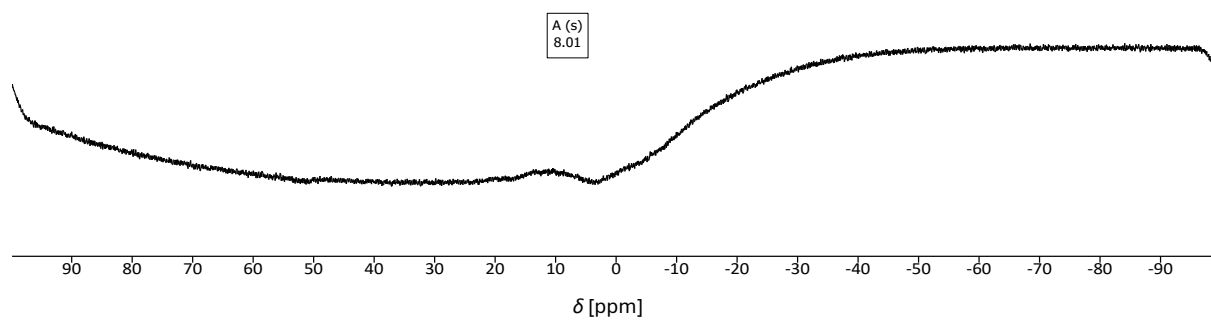**Figure S38** ¹H NMR of a solution of **4**·3Py in C₆D₆ (500 MHz, 298 K).

Figure S39 ¹¹B NMR of a solution of **4**·3Py in C₆D₆ (160 MHz, 298 K, note that the signal is strongly broadened, due to a fast exchange of pyridine).
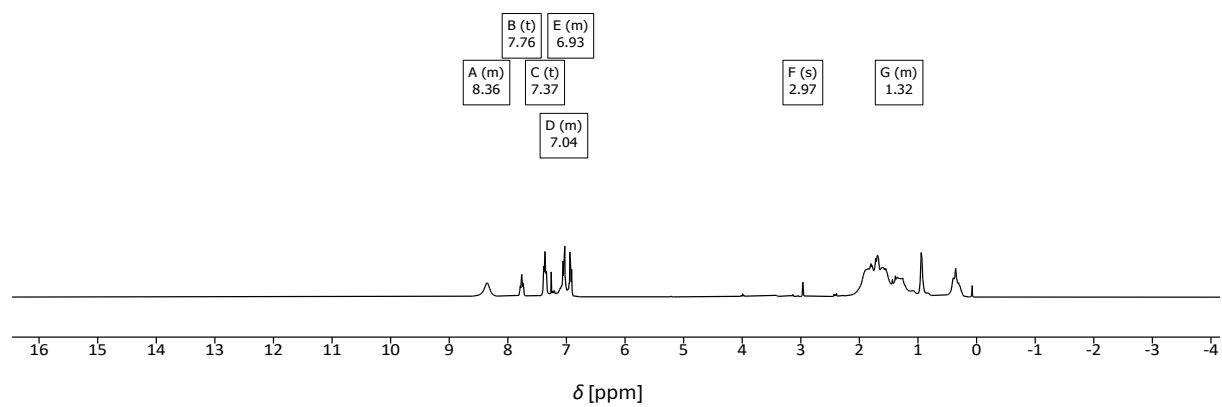

Figure S40 ¹H NMR of a solution of **5**·3Py in CDCl₃ (500 MHz, 298 K).
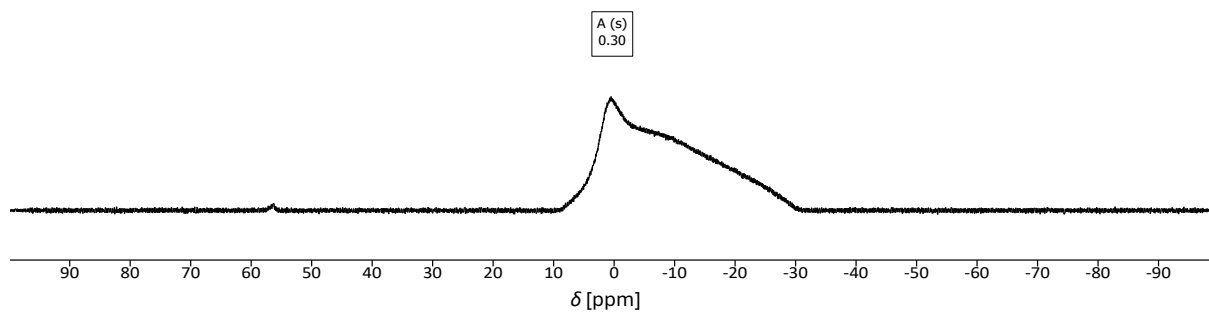
Figure S41 ^{11}B NMR of a solution of **5**·3Py in CDCl$_3$ (160 MHz, 298 K).
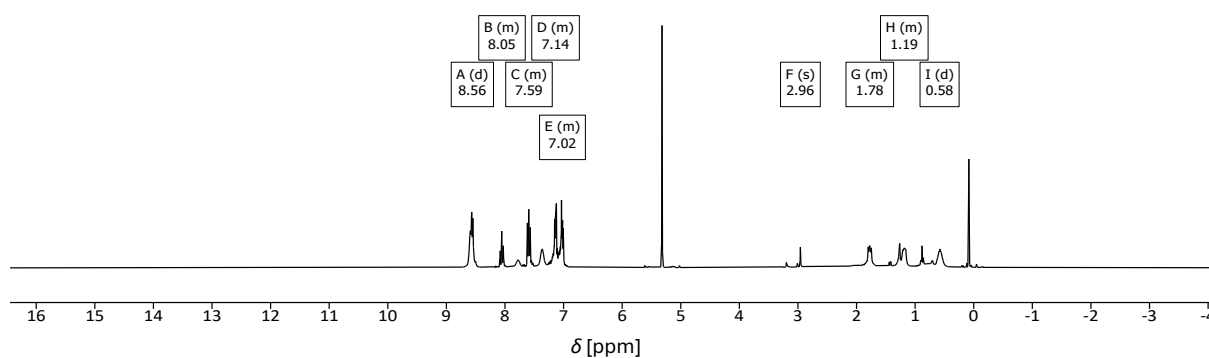
Figure S42 ^{1}H NMR of a solution of **6**·3Py in CD$_2$Cl$_2$ (300 MHz, 298 K).
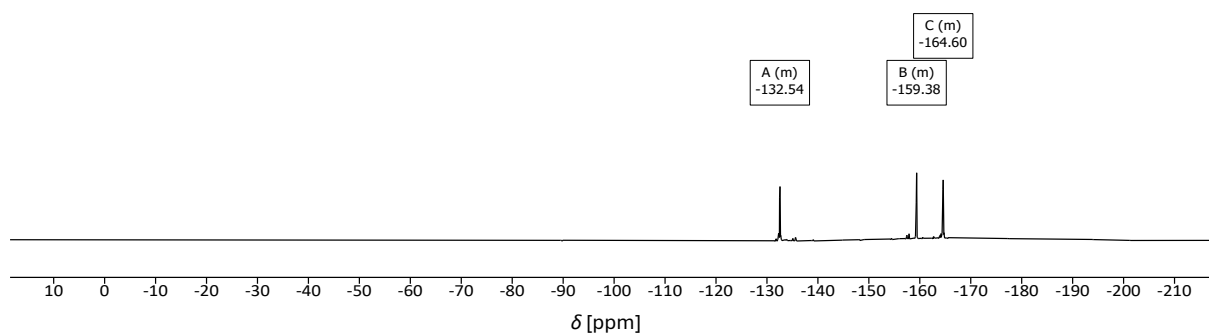
Figure S43 ^{19}F NMR of a solution of **6**·3Py in CD$_2$Cl$_2$ (282 MHz, 298 K).
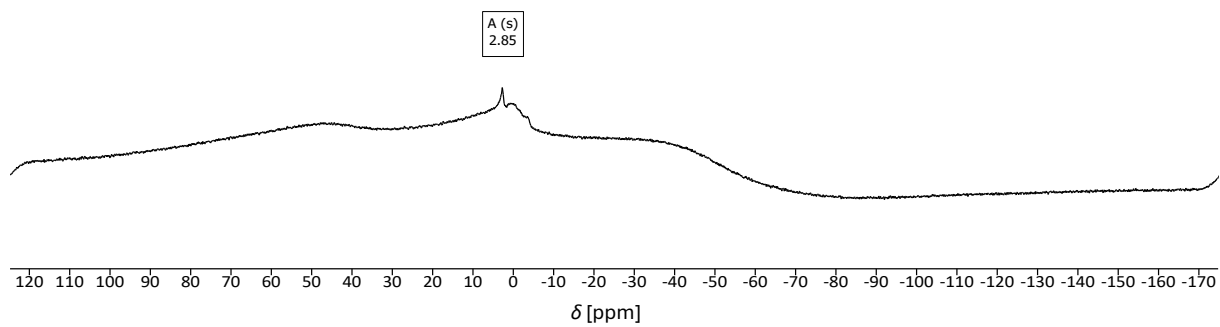
Figure S44 ^{11}B NMR of a solution of **6**·3Py in CD$_2$Cl$_2$ (96 MHz, 298 K).
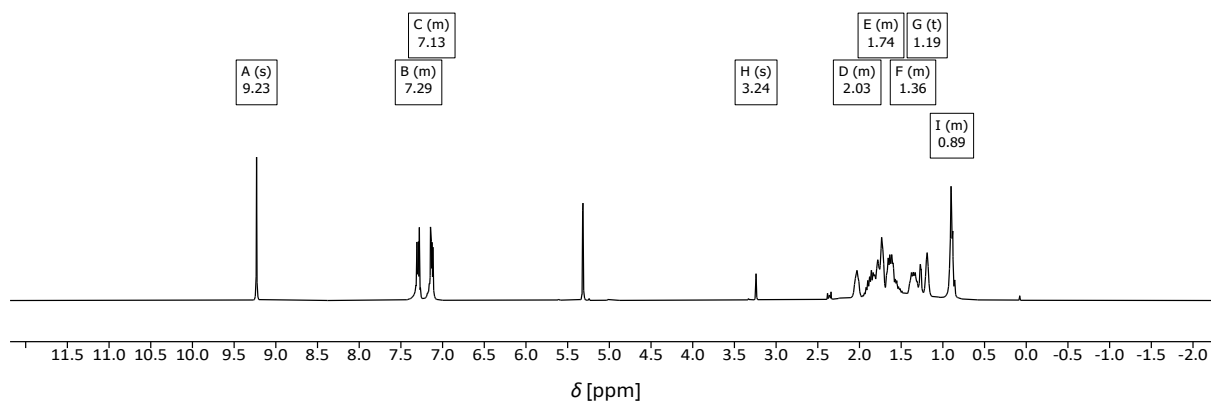
Figure S45 ^{1}H NMR of a solution of **5**·triazine in CD$_2$Cl$_2$ (300 MHz, 298 K).
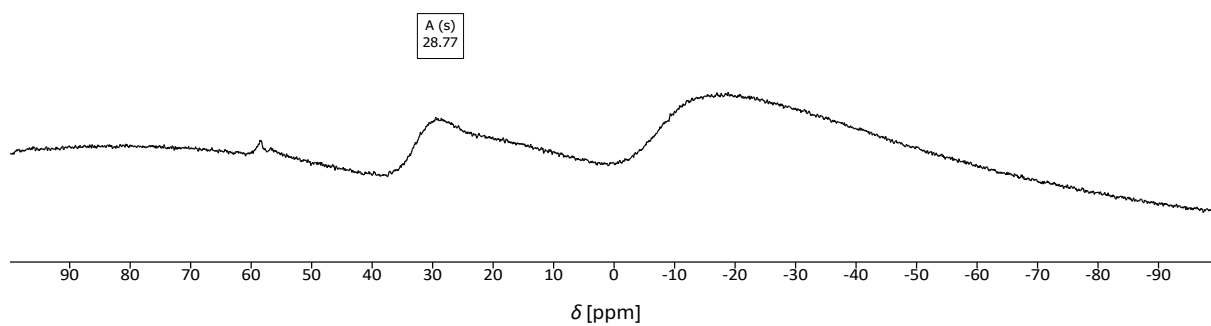
Figure S46 ^{11}B NMR of a solution of **5**·triazine in CD$_2$Cl$_2$ (96 MHz, 298 K).
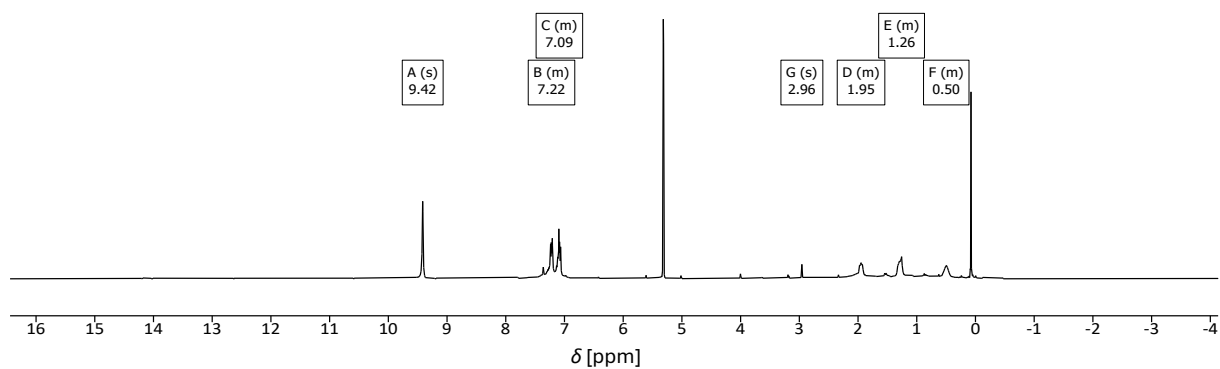
Figure S47 ¹H NMR spectrum of a solution of **6**·triazine in CD₂Cl₂ (300 MHz, 298 K).
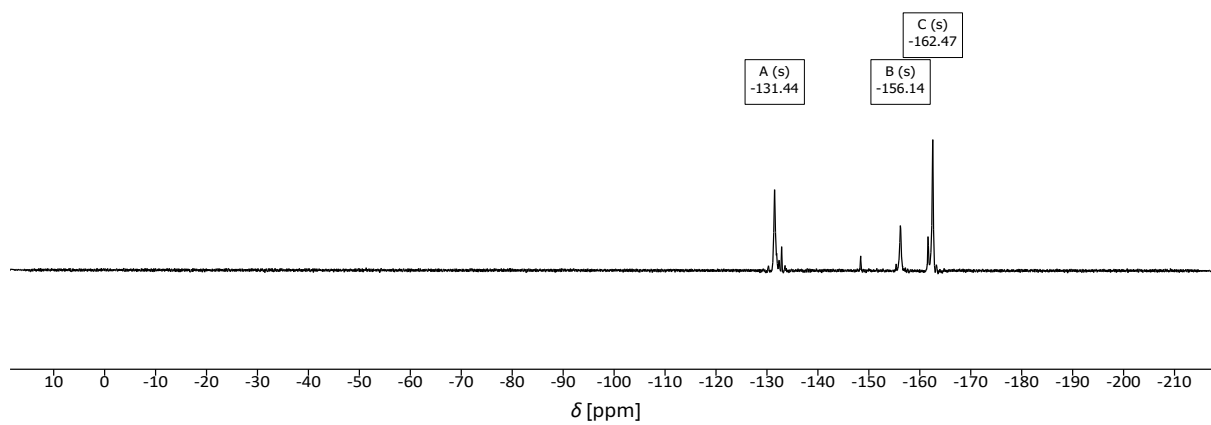
Figure S48 ¹⁹F NMR of a solution of **6**·triazine in CD₂Cl₂ (282 MHz, 298 K).
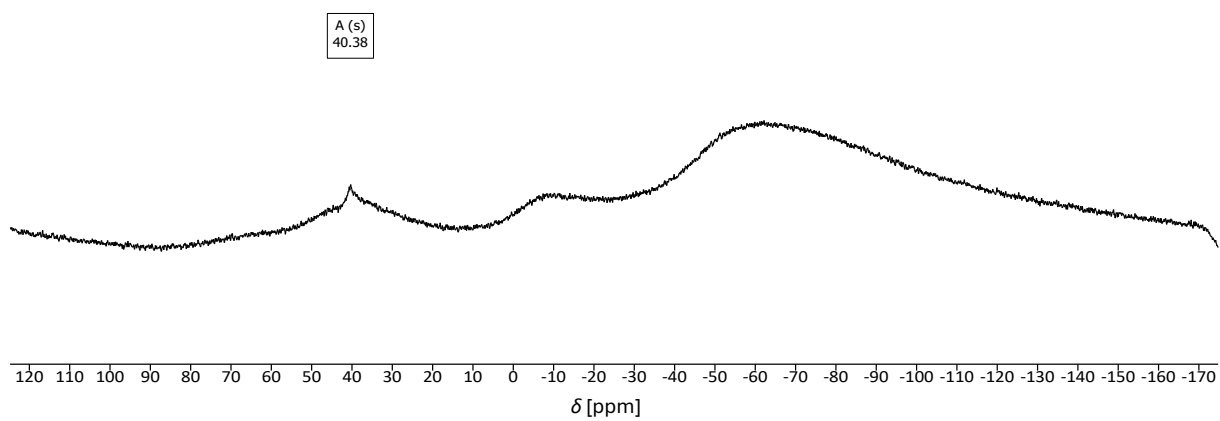
Figure S49 ¹¹B NMR of a solution of **6**·triazine in CD₂Cl₂ (96 MHz, 298 K).
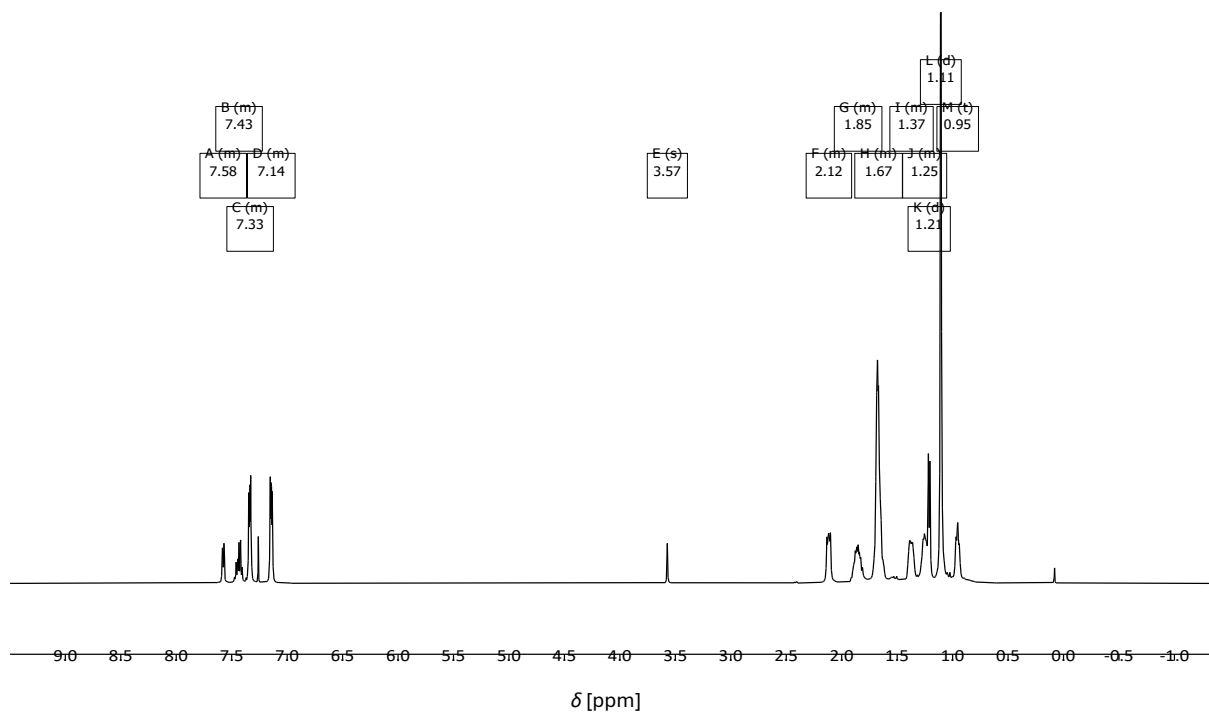
Figure S50 ^{1}H NMR of a solution of **5**·TrisPhos in CDCl$_3$ (500 MHz, 298 K).
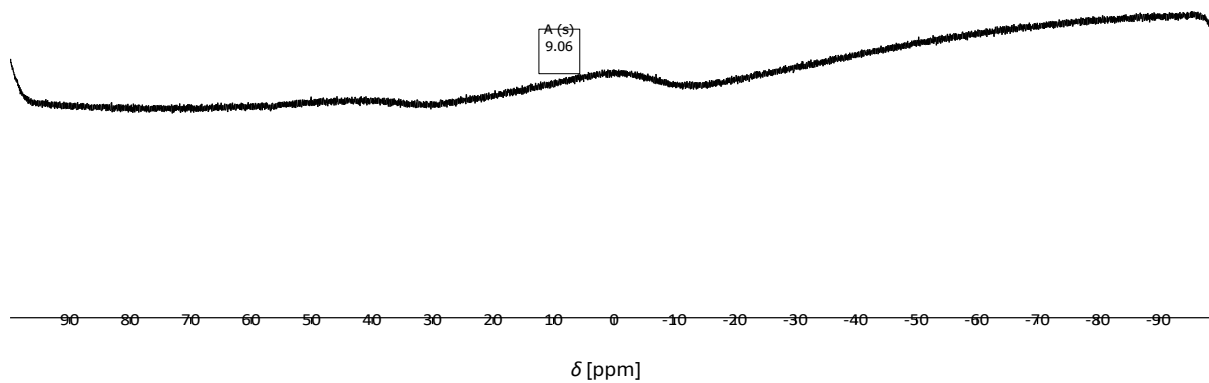
Figure S51 ^{11}B NMR of a solution of **5**·TrisPhos in CDCl$_3$ (160 MHz, 298 K; note, that the signal is broadened, due to a dynamic complexation process).
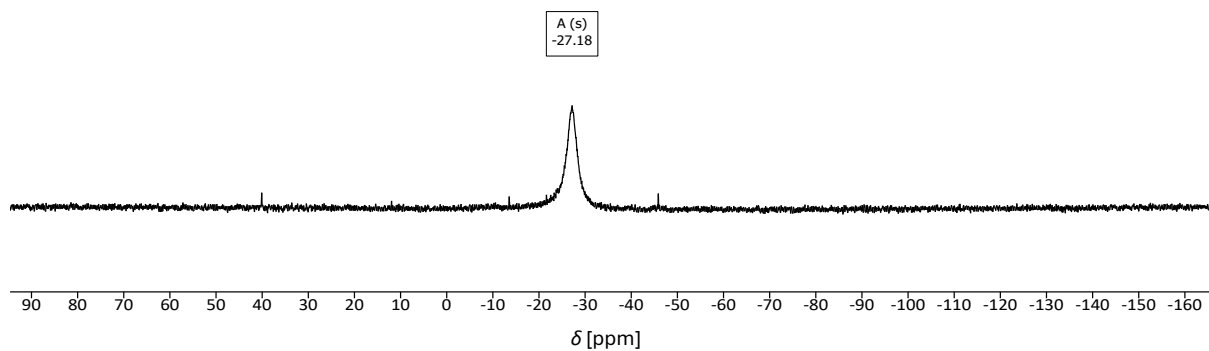
Figure S52 ^{31}P{^{1}H} NMR of a solution of **5**·TrisPhos in CDCl$_3$ (202 MHz, 298 K).
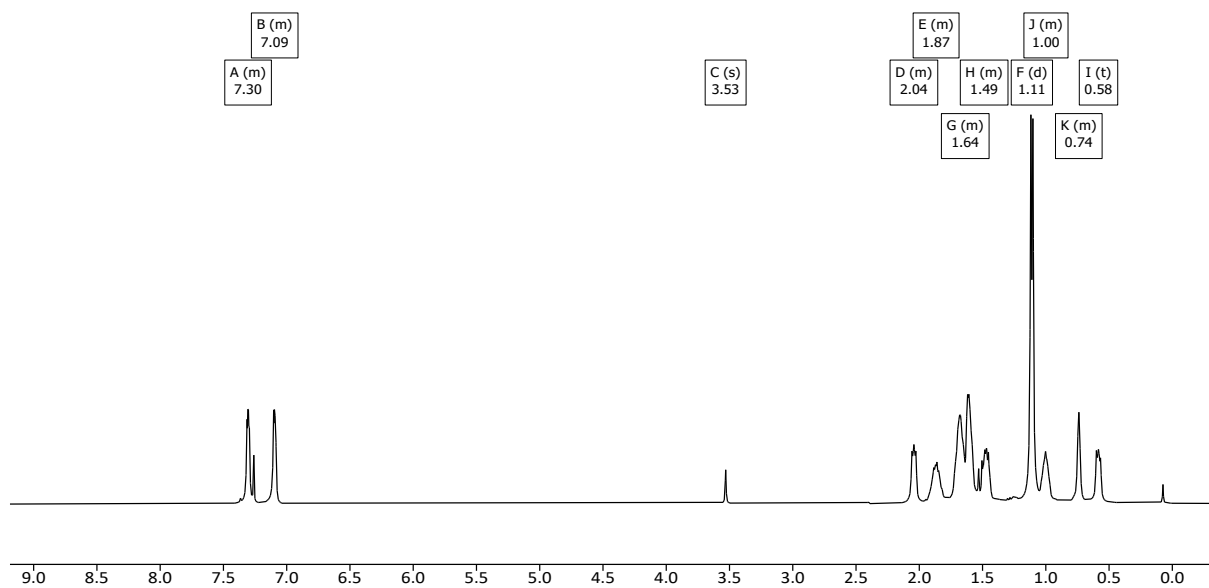
Figure S53 ^{1}H NMR of a solution of **5**·PMe$_3$ in CDCl$_3$ (500 MHz, 298 K).
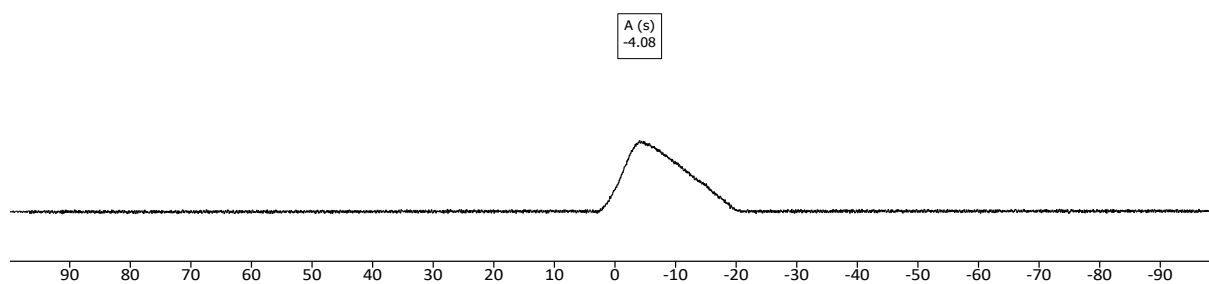
Figure S54 ^{11}B NMR of a solution of **5**·PMe$_3$ in CDCl$_3$ (160 MHz, 298 K)

A (s)
-15.59

140 120 100 80 60 40 20 0 -20 -40 -60 -80 -100 -120 -140 -160 -180
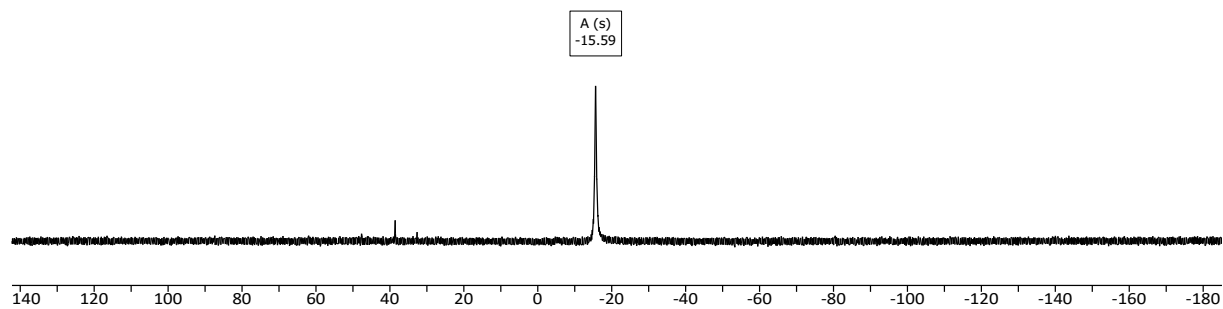
Figure S55 ^{31}P{^{1}H} NMR of a solution of **5**·PMe$_3$ in CDCl$_3$ (202 MHz, 298 K).

X-Ray diffraction experiments

Suitable crystals were obtained by cooling a saturated solution of **2** and **3** in hexane to −30°C or upon concentration of the reaction mixture of **5**·3Py in C_6D_6. The crystals were selected, coated with PARATONE-N oil, mounted on a glass fibre and transferred onto the goniometer of the diffractometer into a cold nitrogen gas stream, which immediately solidifies the oil. Data were collected on a Rigaku SuperNova diffractometer. Using Olex2[S8] the structures were solved with the SHELXT[S9] structure solution program and refined with the SHELXL[S10] refinement package.

CCDC 2345286–2345288 contain the supplementary crystallographic data for this paper. These data can be obtained free of charge from The Cambridge Crystallographic Data Centre via http://www.ccdc.cam.ac.uk/conts/retrieving.html

Figure S56 Molecular structure of **2** in the crystalline state. Displacement ellipsoids are drawn at the 50% probability level. Hydrogen atoms and major disordered parts are omitted for clarity. Selected bond lengths [Å] and angles [°]: C(1)–C(2) 1.563(2), C(2)–C(23) 1.543(2), C(23)–C(24) 1.529(3), Si(1)–C(25) 1.864(2), Si(1)–C(26) 1.870(2), Si(1)–C(27) 1.843(2), Si(1)–Cl(1) 2.084(8); C(25)–Si(1)–Cl(1) 107.2(1), C(26)–Si(1)–Cl(1) 105.5(1), C(27)–Si(1)–Cl(1) 106.4(1).
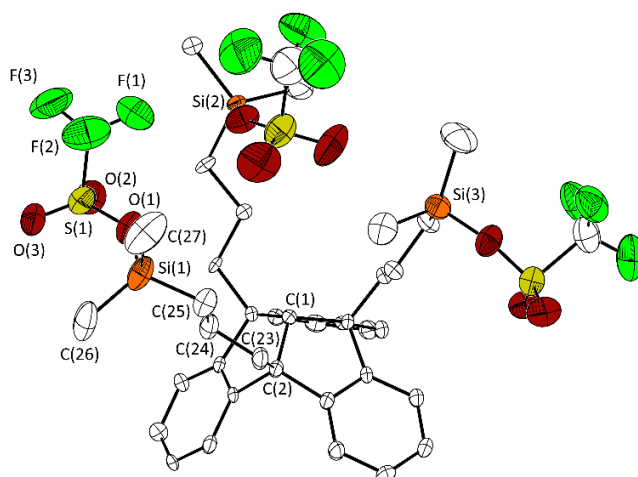
Figure S57 Molecular structure of **3** in the crystalline state. Displacement ellipsoids are drawn at the 50% probability level. Hydrogen atoms and major disordered parts are omitted for clarity. Only one of the two crystallographically independent molecules is shown. For further details, see the ESI.† Selected bond lengths [Å] and angles [°]: C(1)–C(2) 1.562(6), C(2)–C(23) 1.541(7), C(23)–C(24) 1.532(7), C(24)–C(25) 1.520(8), Si(1)–C(25) 1.856(5), Si(1)–C(26) 1.844(9), Si(1)–C(27) 1.842(9) Si(1)–O(1) 1.754(5), O(1)–S(1) 1.522(5); C(25)–Si(1)–O(1) 102.0(3), C(26)–Si(1)–O(1) 109.2(3), C(27)–Si(1)–O(1) 105.4(4).
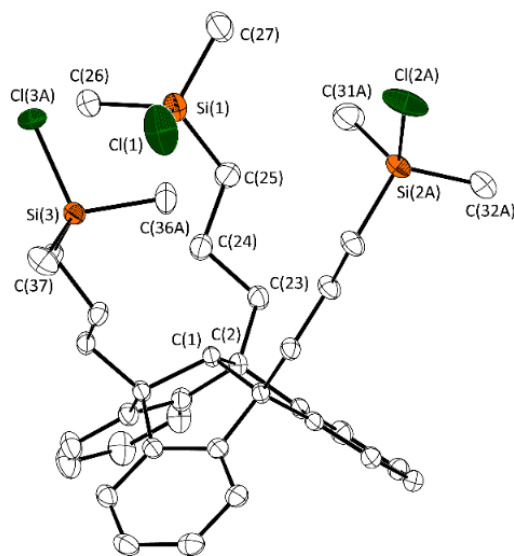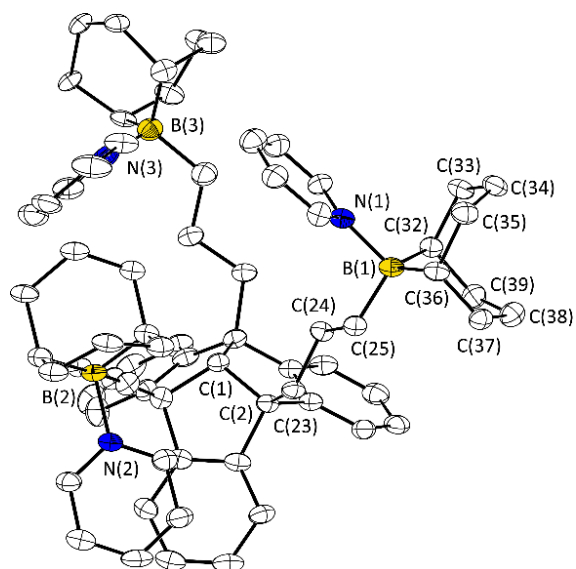
Figure S58 Molecular structures of **5**·3Py in the crystalline state. Displacement ellipsoids are drawn at the 50% probability level. Hydrogen atoms and disordered parts are omitted for clarity. For further details, see the ESI.† Selected bond lengths [Å] and angles [°]: C(1)–C(2) 1.566(7), C(2)–C(23) 1.531(7), C(23)–C(24) 1.524(6), C(24)–C(25) 1.536(6), B(1)–C(25) 1.626(7), B(1)–C(32) 1.626(7), B(1)–C(36) 1.631(7) B(1)–N(1) 1.646(7); C(25)–B(1)–N(1) 104.2(4), C(25)–B1(1)–C(32) 114.9(4), C(25)–B(1)–C(36) 113.4(4), C(32)–B(1)–C(36) 103.9(4). N(1)–B(1)–C(36) 110.0(4).

Table S7 Crystallographic data for the molecular structures of **2**, **3** and **5**·3Py

Parameters	2[a]	3[b]	(5·3Py)·3C$_6$H$_6$[c]
Empirical formula	C$_{37}$H$_{49}$Cl$_3$Si$_3$	C$_{40}$H$_{49}$F$_9$O$_9$S$_3$Si$_3$	C$_{88}$H$_{106}$B$_3$N$_3$
M_r	684.38	1025.24	1238.18
T [K]	100.0(1)	100.0(1)	100.0(1)
Crystal system	monoclinic	monoclinic	monoclinic
Space group	$P2_1/c$	$P2_1/c$	$P2_1$
a [Å]	12.9108(2)	17.6372(6)	12.4550(6)
b [Å]	17.1765(2)	16.1597(5)	11.6294(4)
c [Å]	17.5544(2)	34.9455(11)	25.6412(12)
β [°]	104.341(1)	91.786(3)	98.397(4)
V [Å^3]	3771.60(9)	9955.0(6)	3674.2(3)
Z	4	8	2
ρ_{calc} [g cm^{-3}]	1.205	1.368	1.119
μ [mm^{-1}]	3.287	2.786	0.469
$F(000)$ [e]	1456	4256	1340
Crystal size [mm^3]	0.18 × 0.15 × 0.06	0.37 × 0.043 × 0.031	0.219 × 0.08 × 0.011
Radiation [Å]	Cu Kα (λ = 1.54184)	Cu Kα (λ = 1.54184)	Cu Kα (λ = 1.54184)
2Θ range for data collection [°]	7.066 to 153.05	6.026 to 136.502	6.97 to 153.182
Index ranges	−13 ≤ h ≤ 16, −21 ≤ k ≤ 21, −21 ≤ l ≤ 17	−20 ≤ h ≤ 21, −19 ≤ k ≤ 17, −42 ≤ l ≤ 31	−14 ≤ h ≤ 15, −14 ≤ k ≤ 14, −32 ≤ l ≤ 31
Reflections collected	34291	71522	36522
Independent reflections	7822 [R_{int} = 0.0364, R_{sigma} = 0.0322]	18213 [R_{int} = 0.0813, R_{sigma} = 0.0615]	15024 [R_{int} = 0.0570, R_{sigma} = 0.0768]
Reflections with $I > 2\sigma(I)$	7061	12624	12498
Data/restraints/parameters	7822/0/423	18213/1340/1375	15024/230/1009
Goodness-of-fit on F^2	1.042	1.037	1.084
Final R indexes [$I > 2\sigma(I)$]	R_1 = 0.453, wR_2 = 0.1243	R_1 = 0.0988, wR_2 = 0.2465	R_1 = 0.0756, wR_2 = 0.1569
Final R indexes [all data]	R_1 = 0.0498, wR_2 = 0.1294	R_1 = 0.1289, wR_2 = 0.2682	R_1 = 0.0918, wR_2 = 0.1677
Largest diff. peak/hole [e Å^{-3}]	0.90/−0.99	1.37/-0.66	0.23/-0.30
Flack parameter	–	–	0.4(10)
CCDC number	2345286	2345287	2345288

[a] Disorder of Si(2), Cl(2), C(31), and C(32) over two sites (91:9). Disorder of Cl(3) and C(36) over two sites in ratio 66:34.

[b] Low diffraction power of the crystal because of concerted disorder of four triflate ligands over two sites with ratio 78:22. Lower occupied parts were refined as rigid group using a triflate fragment of CCDC 693002. All disordered atoms were restrained using SIMU, RIGU and ISOR to obtain physically reasonable results. All disordered oxygen and carbon atoms with distances below 0.5 Å between each other were constrained to have equivalent thermal parameters.

[c] Disorder of one BBN, one pyridine and one solvent benzene molecule with ratio 55:45. Refined as inversion twin, ratio 6:4.

References

S1   (a) R. Mills, *J. Phys. Chem.*, 1973, **77**, 685; (b) W. S. Price, H. Ide, Y. Arata, *J. Phys. Chem. A*, 1999, **103**, 448.

S2   A. Macchioni, G. C. Zuccaccia, D. Zuccaccia, *Chem. Soc. Rev.*, 2008, **37**, 479.

S3   H.-C. Chen and S.-H. Chen, *J. Phys Chem.* 1984, **88**, 5118.

S4   Y. H. Zhao, M. H. Abraham, A. M. Zissimos, *J. Org. Chem.*, 2003, **68**, 7368.

S5   M. Mantina, A. C. Chamberlin, R. Valero, C. J. Cramer, D. G. Truhlar, *J. Phys. Chem. A*, 2009, **113**, 5806.

S6   F. Perrin, *J. Phys. Radium*, 1936, **7**, 1.

S7   R. A. Clará, A. C. Gómez Marigliano, D. Morales, H. N. Sólimo, *J. Chem. Eng. Data*, 2010, **55**, 5862.

S8   O. V. Dolomanov, L. J. Bourhis, R. J. Gildea, J. A. K. Howard, H. Puschmann, *J. Appl. Crystallogr.*, 2009, **42**, 339.

S9   (a) G. M. Sheldrick, *Acta Crystallogr., Sect. A* 2008, **64**, 112, (b) G. M. Sheldrick, *Acta Crystallogr., Sect. A* 2015, **71**, 3.

S10 G. M. Sheldrick, *Acta Crystallogr., Sect. C* 2015, **71**, 3.